

**Aus der Universitätsklinik für Zahn-, Mund-, und  
Kieferheilkunde Tübingen  
Poliklinik für Zahnärztliche Prothetik mit Propädeutik**

**Comparative Analysis of  
Additive Manufacturing Methods  
to fabricate  
Auricular Prostheses**

**Inaugural-Dissertation  
zur Erlangung des Doktorgrades  
der Zahnheilkunde**

**der Medizinischen Fakultät  
der Eberhard Karls Universität  
zu Tübingen**

**vorgelegt von  
Unkovskiy, Alexey Sergejewitsch**

**2017**

**Dekan: Professor Dr. I.B. Autenrieth**

**1. Berichterstatter: Privatdozentin Dr. E. Engel**

**2. Berichterstatter: Professor Dr. J. Setz**

**Tag der Disputation: 15.03.2017**

*Dedicated to Mrs. Tatiana Unkovskaya*

*– loving mother, senior colleague and a huge friend of mine*

# TABLE OF CONTENTS

<b>FIGURES</b> .....	<b>6</b>
<b>TABLES</b> .....	<b>7</b>
<b>ABBREVIATIONS</b> .....	<b>8</b>
<b>1 INTRODUCTION</b> .....	<b>9</b>
1.1 REHABILITATION OF PATIENTS WITH FACIAL DISFIGUREMENTS .....	9
1.2 PROSTHETIC APPROACH .....	9
1.3 DIGITAL DATA ACQUISITION. METHODS OF 3D IMAGING .....	11
1.4 MODELLING OF PROSTHESIS CONSTRUCTION .....	12
1.5 ADDITIVE MANUFACTURING AND RAPID PROTOTYPING .....	13
1.5.1 Stereolithography .....	13
1.5.2 Fused deposition modelling .....	14
1.5.3 Selective laser sintering .....	14
1.6 PRODUCTION OF A DEFINITIVE PROSTHESIS .....	14
1.7 INVESTIGATION OF AM METHODS EMPLOYED FOR FACIAL PROSTHESES MANUFACTURING .....	17
1.8 MAIN GOALS AND HYPOTHESES OF THE STUDY: .....	19
<b>2 MATERIALS AND METHODS</b> .....	<b>20</b>
2.1 DESIGN OF THE STUDY & PARTICIPANTS .....	20
2.1.1 Calculation of sample size (number of participants) .....	20
2.1.2 Ethical approval and recruiting .....	20
2.2 BRIEF OVERVIEW TO THE STUDY MEASURES: IN VIVO AND IN VITRO .....	21
2.3 ANTHROPOMETRY AND DIGITALIZATION .....	23
2.3.1 Anthropometry & measurements in vivo .....	23
2.3.2 Structured light scanning, postprocessing, and digital measuring .....	27
2.3.3 Distance measurements in the CAD software .....	31
2.3.4 CAD Modelling .....	31
2.3.5 Additive manufacturing .....	32
2.4 QUANTITATIVE ANALYSIS OF DIMENSIONAL ACCURACY .....	34
2.4.1 Definition of data sets and data groups .....	34
2.4.2 Preparing the Datasets .....	34
2.4.3 Calculation of the measurement error .....	35
2.4.4 Comparing data groups .....	35
2.5 QUALITATIVE ANALYSIS OF SKIN TEXTURE REPRODUCTION .....	36
2.5.1 Reference areas for analysis .....	36
2.5.2 Stereomicroscopy .....	37
2.5.3 Profilometry .....	37
<b>3 RESULTS</b> .....	<b>38</b>
3.1 PARTICIPANTS AND MEASUREMENTS .....	38
3.1.1 Missing measurements .....	38
3.1.2 Calculation of measurement error .....	39
3.1.3 Mean differences towards the reference .....	40
3.2 SKIN SURFACE ANALYSIS .....	47
3.2.1 Visual analysis of the surface .....	47
3.2.2 Profilometry .....	49
3.3 PRODUCTION COSTS AND TIME .....	51
<b>4 DISCUSSION</b> .....	<b>52</b>
4.1 DISCUSSION OF APPLIED METHODS .....	52
4.1.1 Proband and recruiting .....	52
4.1.2 Data acquisition/ scanning of ears/ digitalisation .....	52
4.1.3 Measurements and measurement error .....	53
4.1.4 Manufacturing methods .....	54

4.2	RESULTS: DIMENSIONAL ACCURACY.....	55
4.2.1	<i>Comparison of in vivo data group to AM measurements: clinical relevance.....</i>	55
4.2.2	<i>Comparison of CAD dataset to AM measurements.....</i>	55
4.2.3	<i>Similar studies to the topic.....</i>	57
4.3	RESULTS: SURFACE STRUCTURE .....	58
4.4	THE POTENTIAL OBJECTIVES FOR FURTHER INVESTIGATIONS TO THE TOPIC.....	60
<b>5</b>	<b>CONCLUSION .....</b>	<b>61</b>
<b>6</b>	<b>SUMMARY .....</b>	<b>62</b>
<b>7</b>	<b>SUPPLEMENT .....</b>	<b>64</b>
7.1	ATTACHEMENT 1. SAMPLE SIZE FOR COMPARING THE AM METHODS.....	64
<b>8</b>	<b>ZUSAMMENFASSUNG .....</b>	<b>66</b>
8.1	EINLEITUNG.....	66
8.1.1	<i>Genauigkeit der AM Methoden .....</i>	67
8.1.2	<i>Reproduzierbarkeit der Hautstruktur .....</i>	68
8.1.3	<i>Zweck der Studie .....</i>	69
8.1.4	<i>Ziel der Studie .....</i>	69
8.1.5	<i>Wissenschaftliche Hypothesen .....</i>	69
8.2	PROBANDEN, MATERIALEN UND METHODEN .....	69
8.2.1	<i>Rekrutierung und Erfassung von Probanden (in vivo).....</i>	70
8.2.2	<i>Produktionsphase.....</i>	70
8.2.3	<i>Referenzmessung (CAD, STL, FDM, SL).....</i>	70
8.2.4	<i>Statistische Methode.....</i>	70
8.2.5	<i>Hautstruktur .....</i>	71
8.3	ERGEBNISSE.....	71
<b>9</b>	<b>PUBLICATIONS .....</b>	<b>73</b>
<b>10</b>	<b>REFERENCE.....</b>	<b>74</b>
<b>11</b>	<b>DECLARATION OF THE OWN SHARE TO THIS STUDY .....</b>	<b>81</b>
<b>12</b>	<b>ACKNOLEDGMENTS .....</b>	<b>83</b>
<b>13</b>	<b>CURRICULUM VITAE.....</b>	<b>84</b>

## FIGURES

Figure 1 Conventional and digital workflows of facial prostheses manufacturing. Various approaches of AM utilization.....	15
Figure 2. Overview of the study measures. 7 digitalizations resulted in inferior quality which hinders evaluation process and further additive manufacturing. Thus, the corresponding 7 datasets of ear anthropometry were excluded.....	22
Figure 3. Localization of the landmarks with accordance to the selected anthropometrical approach used (see Tables 1, 2 on pages 1,1) .....	24
Figure 4. Landmarks pointed out on the ear surface with accordance to the anthropometrical approach used.....	24
Figure 5. Attaching the metal balls of 1 mm in diameter on their places according to the anthropometrical approach used.....	26
Figure 6. The process of structured light scanning with the hand-held Artec Spider scanner. The scanner is moved around the area of interest under constant control of the software depicting the acquisition in real-life format (also see Figure 7 on page 29).....	27
Figure 7. Pathway of the scanning process: A to B (left) to scan the posterior inner pinna (red areas); continuously moving from B to C (middle) to scan the Helix and anterior inner pinna; and from C to D (right) to scan the rear part of the outer ear. This scanning process was performed 3 times to create 3 data sets.....	28
Figure 8 3D-images of the participant's auricle in OBJ format in Artec Studio software .....	29
Figure 9. Post-processing chain including the settings for each of the 23 enrolled EpiRP cases to obtain images in OBJ format .....	30
Figure 10 Distance measurement in the CAD software with the "digital lineal" tool....	31
Figure 11. 3D model of the ear APR after being edited in the CAD-software and ready for the further AM-process .....	32
Figure 12. APRs manufactured respectively with SLS, SL, and FDM methods .....	32
Figure 13. Stone cast of one of the probands to measure the surface roughness .....	36
Figure 14. Location of the wrinkles to be examined with the use of profilometry .....	37
Figure 15. Mean absolute differences (Bland and Altman plot) of in vivo measurements compared towards measurements of 23 SLS, 23 FDM and 11 SL APRs and towards CAD measurements. Each colour of the line represents respectively the groups of measurements listed in table 5 on page 40. The shaded area around the black reference line (0) indicated the 2 mm deviation of clinical relevance.....	42
Figure 16. Mean absolute differences (Bland and Altman plot) of CAD measurements compared towards measurements of 23 SLS, 23 FDM and 11 SL APRs. Each colour of the line represents respectively the groups of measurements listed in table 6. The shaded area around the black reference line (0) indicated the 2 mm deviation of clinical relevance.....	43
Figure 17. Mean relative differences (Bland and Altman plot) of in vivo measurements compared towards measurements of 23 SLS, 23 FDM and 11 SL APRs. Each colour of the line represents respectively the groups of measurements. The shaded area around the black reference line (0) indicated the 1.5% deviation of statistical relevance.....	45

Figure 18. Mean relative differences (Bland and Altman plot) of in vivo measurements compared towards measurements of 23 SLS, 23 FDM and 11 SL APRs. Each colour of the line represents respectively the groups of measurements. The shaded area around the black reference line (0) indicated the 1.5 % deviation of statistical relevance ..... 46

Figure 19. Stereomicroscopy of three FDM-, SLS-, SL-produced APRs and one stone cast with the 16x enlargement ..... 48

Figure 20. Stereomicroscopy of three FDM-, SLS-, SL-produced APRs and one stone cast in "Lobula" area with the 10x enlargement. 1- "Lobula basis"; 2 – "Lobula corpus" ..... 48

Figure 21 "Helix" area on the three-dimensional image, AM methods have addressed to. The wrinkle "Helix" is not captured. .... 49

Figure 22. Profile graphics of the three "Lobula basis" wrinkle of gypsum model (black line), SLS-produced APR (orange line), FDM-produced APR (green line) and SL-produced APR (blue line). None of the lines is similar to the referent black one.. 50

## TABLES

Table 1. Anatomical landmarks, their abbreviations, and localizations with accordance to the anthropometrical approach ..... 25

Table 2. Sections of measurements used in the selected anthropometrical approach .... 26

Table 3. Features of AM methods utilization ..... 33

Table 4. Measurement error (ME) within the data groups. The cells contain the number (n, first row) of measurements available within one data group for each section of measurement. The second row in each cell shows the calculated value of mean measurements and the SD. The third row contains the measurement error of the single measurements. The last row of the table contains the mean value of the measurement error within the data group. .... 39

Table 5. Mean differences (Biases) of in vivo and CAD measurements compared towards measurements on the 23 SLS, 23 FDM, and 11 SL APRs. A cell contains the number of mean measurements (n), the mean difference towards the CAD measurement followed by the minimum and maximum value of bias..... 40

Table 6. Mean relative differences of AM methods compared to in vivo and CAD measurements. The highest values are marked with the red colour, the lowest with – green. Total mean is calculated with (all) and without (w/o) short distances due to the measurement bias/missing values of short distances..... 44

Table 7. Mean (Pt) values of the reference wrinkles ..... 49

Table 8. Summary of other studies on the topic of dimensional accuracy of AM methods ..... 57

## ABBREVIATIONS

3D	Three-dimensional
ABS	Acrylnitril-butadien-styrol
AM	Additive manufacturing
CAD	Computer aided design
CAM	Computer aided manufacturing
CNC	Computerized numerical control (milling)
DICOM	Digital imaging and communication in medicine (data format)
FDM	Fused deposition modelling
OBJ	Object (data format)
PLA	Polylactic acid
RM	Rapid manufacturing
RP	Rapid prototyping
RT	Rapid tooling
SLS	Selective laser sintering
SL	Stereolithography
STL	Solid-to-layer (data format)

### Anthropometrical landmarks:

Sa	Supraaurale
Sba	Subaurale
Pra	Preaurale
Pa	Postaurale
Obs	Otobasion superior
Obi	Otobasion inferior
Tra	Tragus
Ah	Antihelix
Sa'	Point sa'
Sba'	Point sba'
Pa'	Point pa'



# 1 INTRODUCTION

## 1.1 Rehabilitation of patients with facial disfigurements

Rehabilitation of patients with disfiguring facial injuries heads to restore the volume of the lost tissue, its function as well as the physical appearance of the face [67].

With regard to auricular prostheses two objectives of rehabilitations have to be taken into account [65]:

- Aesthetically: to conceal the mutilation and make the prostheses mostly invisible
- Functionally: to provide a better hearing.

For decades various surgical techniques have been attempted to master auricular disfigurements including tissue engineering [76, 77]. However, the unpredictability of the aesthetical outcome was always considered as a main limitation of the surgical approach [34, 43]. The rehabilitation of facial disfigurements by means of prosthetic appliances has been reported as advantageous to surgical reconstruction using autogenous flaps [34, 38, 83]. Such prosthetic solutions can be applied as “auricular prostheses” to patients having their pinna totally or partially lost.

## 1.2 Prosthetic approach

Conventionally, the prosthetic approach of treating patients, missing any part of the face includes a few fundamental stages, [6, 67, 69, 72, 80],

namely:

- impression taking of the afflicted area
- wax up and its try-in on the patient together with determination of the primary colour of the skin
- fabrication of the mold
- processing of the prosthesis material and its final coloration.

Due to advancements in the medical field some stages of the conventional method were described as being easily superseded by means of computer technologies. A considerable number of new prosthetic approaches referring to computer-aided design (CAD) and computer-aided manufacturing (CAM) were presented, and reproduction of all facial parts by means of new computerized method was reported in a row of studies [20, 29, 33, 39, 57, 66, 79].

The standard protocol of computerized methods of facial prostheses manufacturing includes the following steps:

- 3D imaging of a defect and opposite organ if present
- designing a 3D model of the future prosthesis form
- try-in of the form on the patient
- mold making and production of silicone prosthesis in the same way as the analogue production way described above.

A better precision, efficiency and decreased production time of prostheses manufacturing due to the use of CAD/CAM technologies have been reported [28, 57]. However, some authors [63] found this novel approach demanding in terms of high-cost equipment. Detailed description of digital prostheses manufacturing approach is easier to be given, when going through all stages of the production chain.

### **1.3 Digital data acquisition. Methods of 3D imaging**

Whichever a method of facial prostheses production is chosen, the first stage is to gather the information about the defect and morphology of the afflicted area. For decades alginate, hydrocolloid, and silicone materials have been successfully used. However, the pressure of the material to the wound implied for a patient plenty discomfort and resulted in distortions of the impression [22, 52, 53, 55].

The digital data acquisition has been reported as an alternative to the traditional impression taking [13, 42, 70, 73]. The images obtained either by computer tomography (CT) and magnetic resonance imaging (MRI), or by 3D-stereophotography and surface scanning can be uploaded to special software for the virtual formation of the prosthesis and a 3D reconstruction of the face. The fact that the scanning process is contact-free allows to avoid any pressure on soft tissues, this way providing better accuracy of the surface topography. This is particularly important, when working with areas without any bone support [47, 70].

Traditionally methods of computer tomography (CT) and magnetic resonance imaging (MRI) have been used for digital data acquisition. However, the radiation exposure in case of CT and the need of additional software to convert the data from the DICOM (digital imaging and communication in medicine) format into STL were recognized as their main disadvantages [68].

Surface scanning has also been applied to maxillofacial prosthetics. To this group of imaging methods belong laser scanning, structured light scanning, and stereophotogrammetry. Such methods provide the virtual image in the STL format directly, which is advantageous to CT and MRI.

The main limitation of surface scanning methods is the fact, that a light or laser beam as such is practically just a straight line, which is not able to trace a complex anatomy and therefore to provide data about regions, that are obscured from the light of sight, anatomical cavities for instance. Thus, surface imaging techniques are not able to capture the intricate details of the auricle [59]. To overcome this limitation, the medical crew has to move the scanner over the whole area of interest from different angles so,

that the light or laser beam follows the whole geometry of the object and attains its undercuts. This may be either challenging or unfeasible at all and implies for the patient to be seated and remain motionless for a sustained period (approximately 15-30 min). Additionally, the hair cover was described as a potential hindrance for a good surface imaging [32].

#### **1.4 Modelling of prosthesis construction**

Conventionally, after the information about the defect morphology is gathered, the wax-up of the future prosthesis is carried out by a dental technician manually. It is considered to be a time-consuming and a challenging task [27, 50, 60, 79]. The produced prosthesis form must match normally the contralateral side in terms of shape, size, and position. It is highly dependent on the artistry and skills of the maxillofacial technician. As the use of 3D scanners allows covering much more extended area, providing the data about the topography of the contralateral side, the so-called mirror imaging technique can be opted. The construction of the prosthesis is simply adopted from the opposite facial part and matched to the affected area. The mirror-imaging technique decreases the time of prosthesis construction and allows achieving potentially a better aesthetical outcome [14, 20, 50, 82]. This technique is particularly applicable when dealing with ear defects [1].

Modelling and formation of the future prosthesis construction by means of CAD has been reported as advantageous to the conventional approach in terms of reducing production time, cost and was recognized to cause less discomfort for the patient [89].

As far as the process of the virtual modelling is accomplished, the prosthesis must be somehow transferred from the CAD-software into real live. Traditionally a three-part stone mold is constructed based upon the wax prototype, into which a silicone is later loaded for the casting of the future prosthesis.

Nowadays there are some alternative methods to manufacture the definitive prosthesis, based on its virtual forerunner. The so-called additive manufacturing (AM) was incorporated into the digital workflow of facial prostheses manufacturing [41].

## 1.5 Additive manufacturing and rapid prototyping

AM is recognized as a relatively new technology to produce physical models utilizing the CAD data sources by means of selective solidification of horizontal layers simultaneously with stepwise submergence along the vertical axis [41].

A relatively rapid turnaround time as well as low production costs of the intended product, particularly compared to the conventional manufacturing process have been reported as main advantages to accept the AM as the technology of choice in the medical field [75]. Various approaches of AM utilization have been introduced including “Rapid Manufacturing”, “Rapid Tooling” and finally “Rapid Prototyping” [37, 41].

Utilization of AM was an important step on the way to make treatment planning more precise, subsequently making the final outcomes more predictable.

Technological and industrial advancements contributed to the development of multiple AM techniques, exploiting various materials that are suitable for layered object formation, ranging from liquids and powder to resin filaments, paper, polymers and metals. These materials are in their turn solidified by means of glue, laser or light beam. Such layer-wise and additive method of building up allows to produce models regardless to the complexity of their geometry, taking therefore into consideration all intrinsic anatomical features [5].

Nowadays a big range of AM techniques have been introduced. All of them according to classification of Gebhardt [37, 41] can be divided into five main groups, which is based on various combinations of materials and curing methods. It is not the intension here to speak about the technical features and characteristics of each method. Still three of them that have been frequently employed in maxillofacial prosthetics and for this reason used in this study are worth mentioning.

### 1.5.1 Stereolithography

Stereolithography (SL) is the oldest AM system [48]. It builds models through layer-wise solidifying of a photosensitive resin, which is stored in a special bath [44]. SL

provides the highest geometrical accuracy and the best surface quality among any other AM methods existing today [54]. However, the build-up process may contain layers that greatly overhang the layers below, thus demanding the supporting structures to be applied [64, 85]. With regards to maxillofacial prosthetics SL has been also widely employed, namely for production of prosthesis replicas and surgical guides for implants placing [1, 66].

### *1.5.2 Fused deposition modelling*

Fused deposition modelling (FDM) is based on the same layer-wise principle of additive manufacturing as SL, utilizing plastic filaments instead of a photosensible liquid. Filaments made of acrylonitrile butadiene styrene (ABS) or polylactic acid (PLA) are first molten and then extruded from a fine nozzle [37, 41, 44]. The method of FDM requires supporting structures. Its resolution is known to be relatively poor, compared to SL [54].

### *1.5.3 Selective laser sintering*

Selective laser sintering (SLS) technique utilizes the laser beam for the computer driven solidification of a heat-fusible powder [37, 41]. The fact that SLS doesn't require any supporting structures, as the upcoming layer is sustained by the underlying unsintered powder is the main advantage of SLS compared to other AM methods [5]. Still some post processing is required. It implies the cleaning of the model from the excesses of the unsintered powder, which might be challenging, when getting it out from the undercuts and anatomical cavities.

## **1.6 Production of a definitive prosthesis**

As it was mentioned before, the crucial moment in production of facial prostheses by means of CAD/CAM is to transfer the data from the CAD software to the hardware of CAM machines to provide it with a physical form. A big number of manufacturing protocols have been introduced to deliver a definitive product based on its three-dimensional prototype (Figure 1).

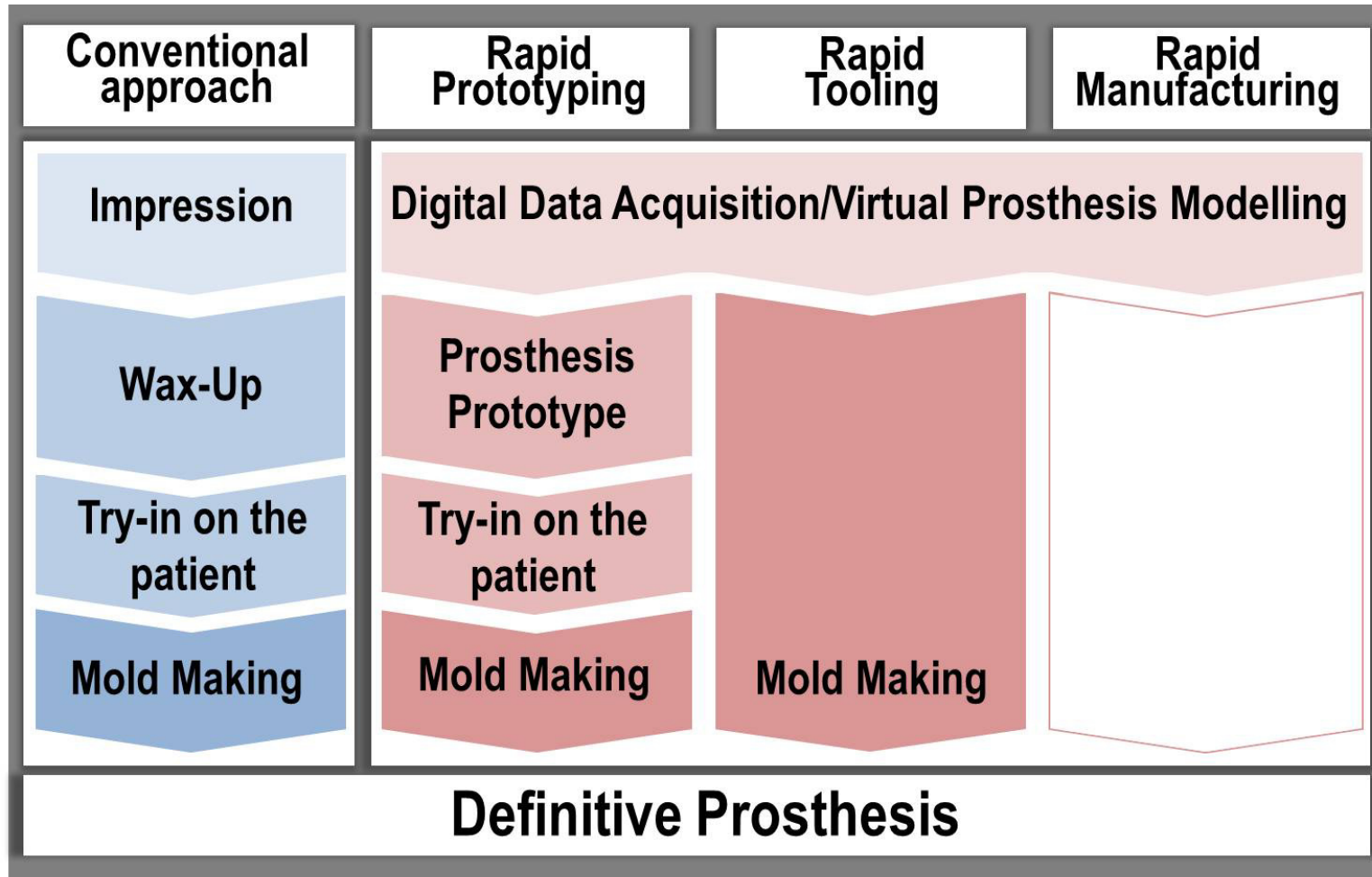


Figure 1 Conventional and digital workflows of facial prostheses manufacturing. Various approaches of AM utilization.

In general, these protocols constitute two main groups: direct printing from silicone, and production of the negative mold, to which a silicone is later on added. The first technique is also known as “Rapid manufacturing” [41] and intends a direct fabrication of the final product without dealing with any prototypes or forerunners. Such approach of AM-methods utilization is beneficial for the production of any objects in industry – [61]. Also in the medical field the “bioprinting” was reported as rapidly developing and promising technology on the way to restore the tissue portions and meeting the functional requirements for transplantation. However little was published about the rapid manufacturing of definitive facial prostheses – the printable maxillofacial silicone is still being developed [51].

With regards to the second group, namely the production of the mold, two approaches can be herein considered, featuring direct and indirect mold making. The first one is also recognized in the technical field as “Rapid tooling”, intending hereby the production of the negative form from the CAD data source for the further multiple fabrication of the final product [41].

In the maxillofacial field this approach implies the direct mold manufacturing by means of AM from CAD data obtained by CT, MRI or surface scanning. The three-dimensional model of the mold can be modelled virtually, being based on the positive form of the primarily constructed prosthesis itself. This approach of direct mold fabrication was pioneered by Cheah in 2003 [12]. Later on a row of authors applied this protocol into clinical practice [19, 29, 57, 81, 89]. The use of various both subtractive [81] and additive manufacturing methods was attempted for the direct mold production. Thus, such AM methods, as SL [66], FDM [17, 18, 29, 46] and 3D-printing [16, 57, 89] have been employed. The mentioned studies revealed the benefits of the introduced protocol that namely are the easiness of mold production, compared to the conventional workflow, and a significantly reduced time for the patient to be present in the clinic, as now try-in of the prosthesis forerunner is intended. The absence of this step means that no alignment of the prosthesis margins to the adjacent tissue and further refinement of its position and shape are performed.



The protocol utilizing AM for the indirect mold making (also known under the widespread definition of “Rapid Prototyping”) implies some additional steps, namely the production of the prosthesis replica (prototype) and its further try-in on the patient. Slight adjustment of the replica in terms of shape, size, matching the contralateral side as well as the alignment of the prosthesis margins to the adjacent tissues are conducted to attain better aesthetics and wearing comfort. These replicas serve afterwards as a positive pattern to produce the negative mold to which the silicone material will be subsequently added. The mold as such is usually produced via silicone rubber molding.

The following AM methods have been commonly used for production of prostheses replicas, ranging from SL [1], FDM [73, 78] and SLS [21, 60, 82, 88] to 3D-printing technology [11, 13, 20, 39, 63, 79, 84]. The use of CNC (computerized numerical control milling) has been also attempted [14].

The study of Cheah et al. [13] compared these two approaches, direct vs indirect mold making, and ascertained their both limitations and advantages. Although the direct mold production was acknowledged as a quicker approach, it leads potentially to higher manufacturing costs. The materials to produce a mold by means of AM are much more expensive compared to silicone in case of silicone rubber molding. However, the fact that the pattern can be refined clinically prior to definitive manufacturing yields potentially in a better aesthetical and functional outcome of rehabilitation.

### **1.7 Investigation of AM methods employed for facial prostheses manufacturing**

Since the AM have been applied to the medicine, various aspects of its use have been analysed. Herein the dimensional accuracy was always considered to be the major concern and was investigated in a row of studies [4, 15, 58].

Literature analysis revealed that the protocol of indirect mold production (RP) has been more frequently used [21, 39, 60, 63, 73]. The literature is mostly comprised of single case studies, just stressing the common benefits of using AM-process for production of facial prosthesis in general, thereby lacking critical evaluation and comparison of each method. No clearness is set, which AM method would rather aid to achieve gains in

efficacy and efficiency in production of facial prostheses, and consequently suits better to be integrated into every day practice.

Nowadays as a result of improvements in soft- and hardware in the field of medical technologies all the main AM processes introduced on the market show a considerably high resolution, which allows manufacturing products with relatively high accuracy. So, the maximal resolution that can be achieved by the method of SL is 0.05 mm, followed by the SLS method with also significantly high resolution of 0.01 mm. The highest resolution of FDM is known to be limited by 0.1 mm [54].

Although the resolution of most AM machines is predetermined and described by the manufacturer, still there are some other error sources that influence the geometrical accuracy. The complexity of anatomy, for instance, must also be considered. The anatomical structures of a human ear have such a complex anatomy - consisting of stiff and flexible areas forming the typical shapes. Reproduction of those parts by means of AM processes might be associated with considerable difficulties, as far as reconstruction of the whole anatomy is concerned. Residual polymerization, creation and removal of supporting structures, laser diameter and surface finishing are among those technical factors, mentioned by Choi (2002), that contribute to model accuracy [15]. Some authors reported, that errors may manifest themselves at any stages of the production workflow, regardless to the AM-technique employed [49, 62]. It means that the initially given resolution of an AM machine might not be the only factor that contributes to the overall production accuracy.

The other issue to be pursued, concerning the application of CAD and AM in maxillofacial prosthetics, is the skin texture reproduction. In the following studies the level of textures detailing that can be recognized visually was ascertained [7, 33]. It was assumed that the minimum detailing level to be reproduced must be 0.1 mm, according to the rating scale of Lemperle [56]. The accuracy of the scanning method used in these studies was reported to be insufficient to reproduce texture details on that level. It must be investigated, whether they in combination with other surface scanning methods might have yielded a better reproduction of the skin texture.

### 1.8 Main goals and hypotheses of the study:

The objective of the present research is to identify the superior AM method in terms of dimensional accuracy and level of the skin texture reproduction to produce auricular prostheses replicas (APRs), using thereby the structured light scanning and rapid prototyping approach.

Therefore following hypotheses have been formulated:

- i.* There exists no difference in the dimensional reproduction of auricular prosthesis replicas made using the three different AM methods (SL, SLS, FDM) compared to the natural ear.
- ii.* There exists no difference in the dimensional reproduction of auricular prosthesis replicas made using the three different AM methods (SL, SLS, FDM) compared to the 3D images of the human ears, the replicas are based on.
- iii.* The SL, SLS and FDM methods in combination with a structured light surface scanner used, enable the successful reproduction of the human ears skin texture on a visually convincing level [56] where the wrinkles starting of the order of 0.1 mm can be visible.
- iv.* Combining the outcomes of hypotheses *i-iii* as well as pricing, a best-in-practice AM method can be identified.

## 2 MATERIALS AND METHODS

### 2.1 Design of the study & participants

This study was designed as anonymous case series with in-vivo measurements (anthropometry) and digital acquisition of one ear with structured light scanning, followed by CAD-modelling, CAD-measurement, APR-production and APR-measurement. Furthermore, one participant was invited to get a silicon impression of one auricle to produce a gold standard gypsum model for qualitative comparison via stereomicroscopy and profilometry.

#### 2.1.1 Calculation of sample size (number of participants)

According to the previous researches on this topic [26, 42], a sample size of at least 17 participants was calculated with “OpenEpi” software [30] to detect a difference of 1.5 %, using an alpha of 5 % and 80 % power (see supplement 1.).

Besides, exceeding 2 mm of difference between APRs and situation in vivo is regarded as clinically relevant difference – [25].

#### 2.1.2 Ethical approval and recruiting

The study protocol, subjects’ information and informed consent sheets were approved by the Ethics Commission of the University Hospital (387/2014BO2) and registered to the German Registry for Clinical Trials (DRKS00007184). All subjects were recruited via a notice and group mail. Thirty volunteers (9 women, 21 men) aged from 18 to 60 years (mean age 37.8 years) were enrolled in the study.

After informed consent and scheduling for the study the participants were assigned with an ID# functioning as a pseudonym: “EpiRP-##”. All datasets were assigned with this ID.

One participant volunteered for the analysis of the surface texture reproduction and consented to impression taking and publication of his documentation/photographs.

The inclusion criteria for all participants were:

- Absence of any ear abnormalities
- Age over 18 y.o.

## **2.2 Brief overview to the study measures: in vivo and in vitro**

First, all participants underwent the procedure of the ear anthropometry including the in vivo measurement of each distance, three times with a digital calliper (see chapter 2.3 on page 23). All study measures including anthropometry and structured light scanning have been performed on the left subjects' auricles.

Secondly, the auricular area, including the pinna was scanned for the digital data acquisition with the use of a portable surface scanner (Artec 3D Spider, Artec Group, Luxembourg, Luxembourg), utilizing the structured light scanning method. After the gathered data was post-processed and converted into OBJ (object) format, it has been transferred to AM machines to produce APRs. The distances of the anthropometrical landmarks were measured within the Software ARTEC Studio, version 9, three times with the "digital lineal".

Thirdly, the distances between the landmarks on each produced APR were measure three times with the digital calliper.

All the gathered values were statistically evaluated with JMP (Version 11.1, SAS Institute Inc., Cary, NC, USA).

The measurements were compared towards measurement bias and the mean differences between in vivo as well as CAD measurements were calculated using the Bland-Altman-Plot [9] (see chapter "Quantitative Analysis of dimensional accuracy" on page 34.

Figure 2 (see below) summarizes the study protocol.

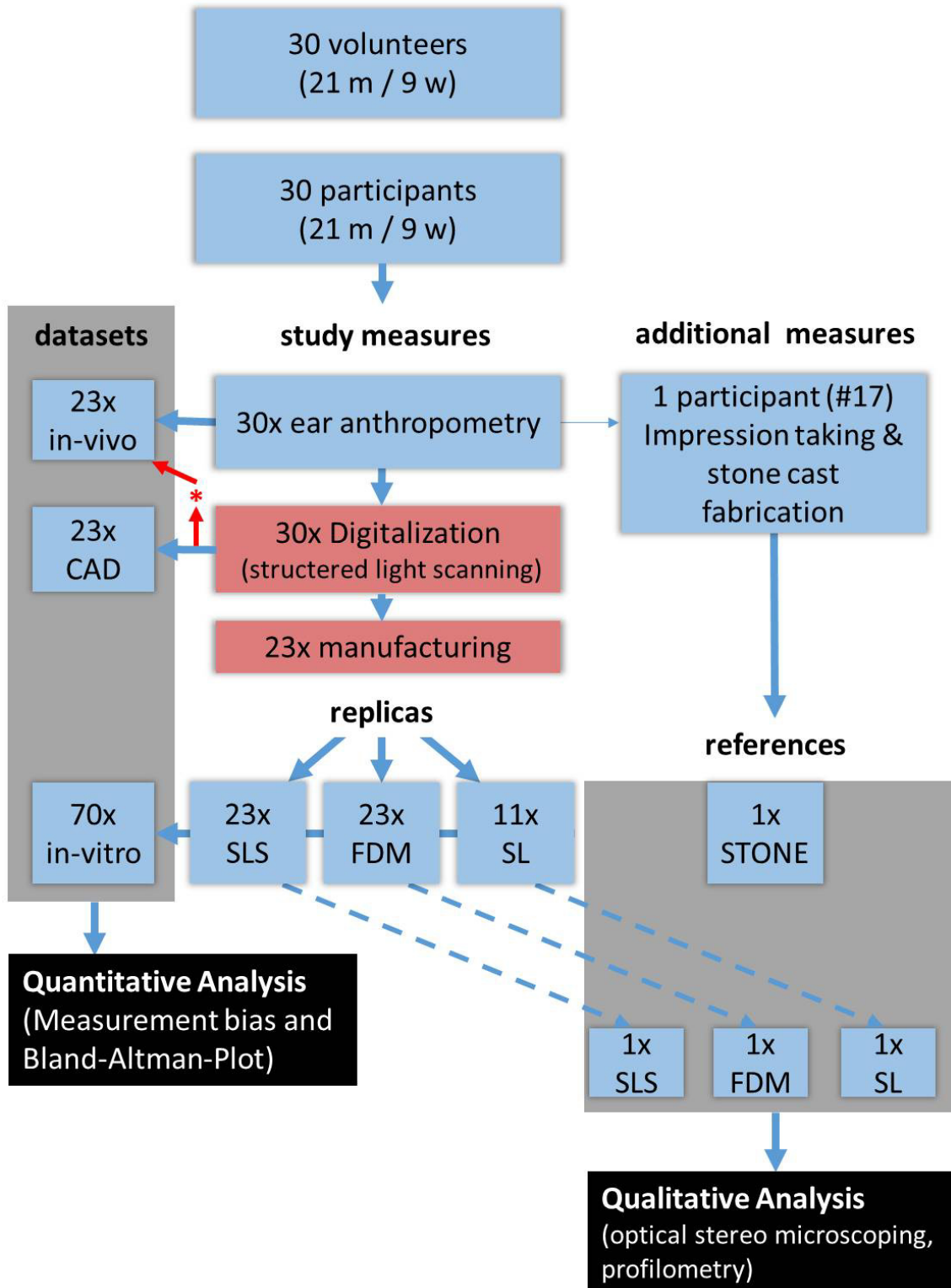


Figure 2. Overview of the study measures. 7 digitalizations resulted in inferior quality which hinders evaluation process and further additive manufacturing. Thus, the corresponding 7 datasets of ear anthropometry were excluded.

## 2.3 Anthropometry and digitalization

### 2.3.1 Anthropometry & measurements *in vivo*

The standard anthropometric landmarks by Farkas [35] and three additional landmarks defined by Coward et al. [23, 26] have been used in the present study (Figure 3 on page 24; Table 1 on page 25).

The subjects were prepared for anthropometry and scanning as follows: first, the auricular area was isolated from the hair, which was covered with a medical cap, which in its turn was secured with an adhesive strip on to the skin in order to prevent dislodging during the measurement procedure (Figure 4 on page 24). Secondly, the skin of the ear was defatted with ethanol 80 %.

Thereafter the landmarks were marked manually on the ear surface, using black permanent marker with 0.78 mm thickness (MULTIMARK 1523 permanent, Faber-Castell, Hamburg, Germany) (Figure 5 on page 26). The distances between the measure points (see Table 2 on page 26) were taken three times with a digital calliper in such way, that the operator never saw the outcome on the display of the calliper, when placing the calliper tips on top of the measuring points. All measurements were performed according to the recommendations for metrology [10]. After completing the analogue measurements metal balls with a diameter of 1 mm  $\pm$  0,05 mm were glued onto the skin using a cosmetic glue (Mastix Spirit Gum, Metamorph GmbH, Berlin, Germany) at exactly the same spots marked with the pencil. Those balls served as reference points for the following light-scanning and digitalization procedures, as they provided the landmarks with volume (Figure 5 on page 26).

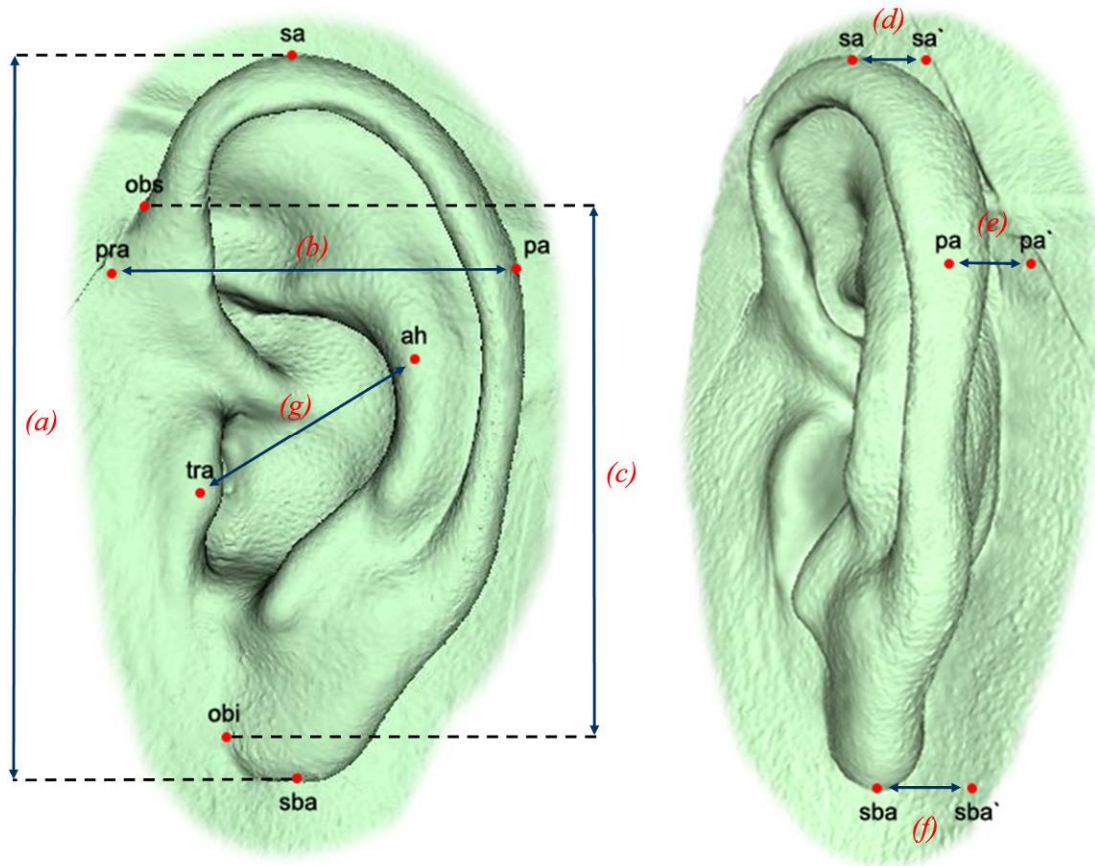


Figure 3. Localization of the landmarks with accordance to the selected anthropometrical approach used (see Tables 1, 2 on pages 25,26)

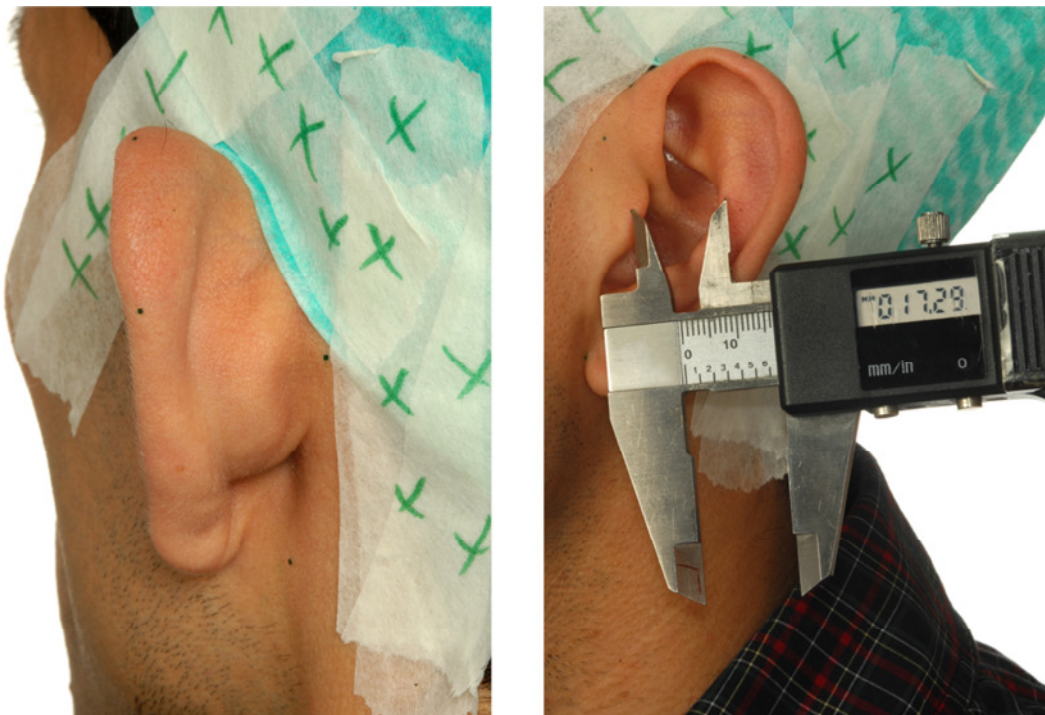


Figure 4. Landmarks pointed out on the ear surface with accordance to the anthropometrical approach used



<b>Landmarks</b>	<b>Abbreviation</b>	<b>Localization of the landmark</b>
<b>Supra-aurale</b>	<b>sa</b>	<i>Highest point of the free margin of auricle</i>
<b>Sub-aurale</b>	<b>sba</b>	<i>Lowest point on the free margin of the earlobe</i>
<b>Pre-aurale</b>	<b>pra</b>	<i>The most anterior point of the ear located just in front of the helix attachment</i>
<b>Post-aurale</b>	<b>pa</b>	<i>The most posterior point of the free margin of the ear</i>
<b>Otobasion superior</b>	<b>obs</b>	<i>Point of attachment of the helix in the temporal region; determines the upper border of ear insertion</i>
<b>Otobasion inferior</b>	<b>obi</b>	<i>Point of attachment of the earlobe to the cheek; determines the lower border of the ear insertion</i>
<b>Tragus</b>	<b>tra</b>	<i>The most vertically outstanding point on the tragus</i>
<b>Antihelix</b>	<b>ah</b>	<i>The most vertically outstanding point on the antihelix</i>
<b>temporal reference of supra-aurale</b>	<b>sa'</b>	<i>Point on side of the head (os temporale) orthogonal from the supra-aurale (sa)</i>
<b>temporal reference of post-aurale</b>	<b>pa'</b>	<i>Point on side of the head (os temporale) orthogonal from the post-aurale (pa)</i>
<b>temporal reference of sub-aurale</b>	<b>sba'</b>	<i>Point on side of the head (os temporale) orthogonal from the sub-aurale (sba)</i>

**Table 1. Anatomical landmarks, their abbreviations, and localizations with accordance to the anthropometrical approach**

Section of measurement	Letter	Description	Classified as
sa-sba	<i>a</i>	Length of the ear	long distances
obs-obi	<i>c</i>	Insertion length of ear	
pa-pra	<i>b</i>	Width of the ear	medium distances
tra-ah	<i>g</i>	Tragus to antihelix	
sa-sa'	<i>d</i>	Clearance between the top of ear and the skin of the os temporale	short distances
pa-pa'	<i>e</i>	Clearance between the most posterior point on the helix and the skin of the os temporale	
sba-sba'	<i>f</i>	Clearance between the lowest point on the free margin of lobe and the skin of the os temporale	

Table 2. Sections of measurements used in the selected anthropometrical approach



Figure 5. Attaching the metal balls of 1 mm in diameter on their places according to the anthropometrical approach used

### 2.3.2 Structured light scanning, postprocessing, and digital measuring

As soon as all metal balls were attached to the marked spots, each participant underwent a scanning process, which was performed with the use of Artec Spider scanner (Artec Group Comp., Luxembourg, Luxembourg). Three recordings of the auricular area including pinna were performed (Figure 6 on page 27). The author followed the recommendations of the manufacturer for Artec scanners after receiving special 1-day training (RSI Technology, Oberursel, Germany).



**Figure 6.** The process of structured light scanning with the hand-held Artec Spider scanner. The scanner is moved around the area of interest under constant control of the software depicting the acquisition in real-life format (also see Figure 7 on page 28).

The author, holding the scanner performed several movements around the area of interest in a certain sequence, as follows from the Figure 7 (see below). The scanning process was not stopped before the full geometry of the auricle and their adjacent tissues have been captured. This approach avoids two major sources of error: first, acquisition of multiple datasets (images) which have to be aligned manually with the software and second, distortions due to the superimposing of the images.

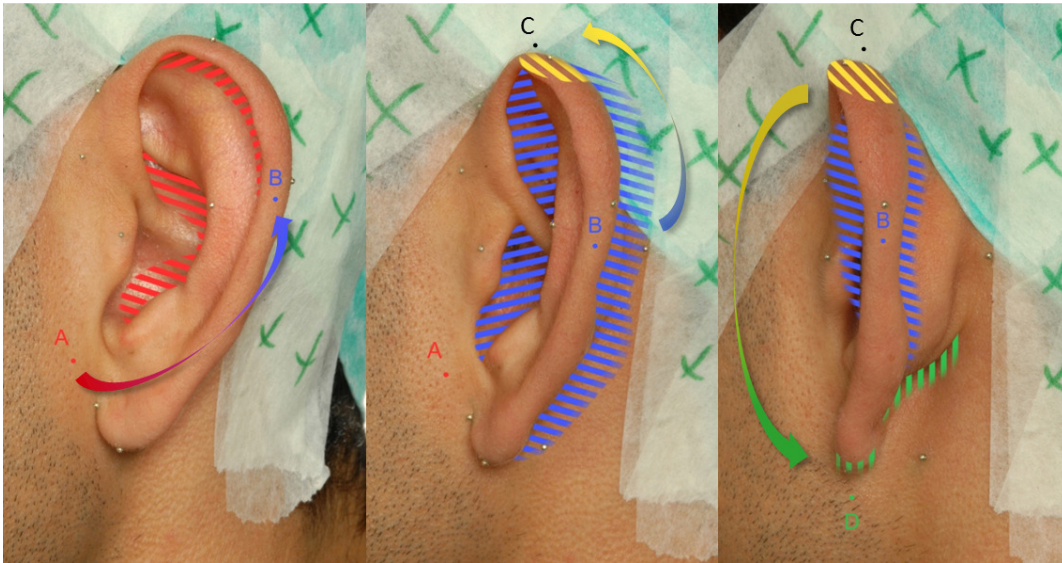


**Figure 7. Pathway of the scanning process:** A to B (left) to scan the posterior inner pinna (red areas); continuously moving from B to C (middle) to scan the Helix and anterior inner pinna; and from C to D (right) to scan the rear part of the outer ear. This scanning process was performed 3 times to create 3 data sets.

The best image was chosen out of the three gathered renderings in the preview mode in the software (ARTEC Studio, ver. 9). The following exclusion criteria were considered:

- presence of any areas of missing data (mostly in undercuts)
- presence of any visible shifting of the anatomical structures (i.e the auricle concha to the tragus area)
- insufficient amount of adjacent tissues captured (around the auricle).

21 review scans of 7 subjects (EpiRP #1, #2, #3, #7, #8, #9, #12) did not meet these requirements and therefore had to be excluded. Thus, datasets of the remaining 23 subjects were used for evaluation and further study measures. The best preview out of

the three gathered images of the remaining 23 subjects underwent the subsequent three stages of post-processing (Figure 9 on page 30).

First, “Global registration”: this stage resulted in a mesh (point of clouds), which in its turn had to be further processed on the screen by means of the computer software.

Secondly, “Sharp fusion”; “Small object filter”; and “Mesh simplification” have been applied. This resulted in the images in STL format. Thereafter the textures were applied and aligned with the existing image and the final 3D image was saved in the OBJ format (Figure 8 – see below). All digital tools applied for the post processing were reported and recommended by the official reseller of Artec products - not hindering/ influencing the dimensional accuracy of investigated objects.



**Figure 8 3D-images of the participant’s auricle in OBJ format in Artec Studio software**



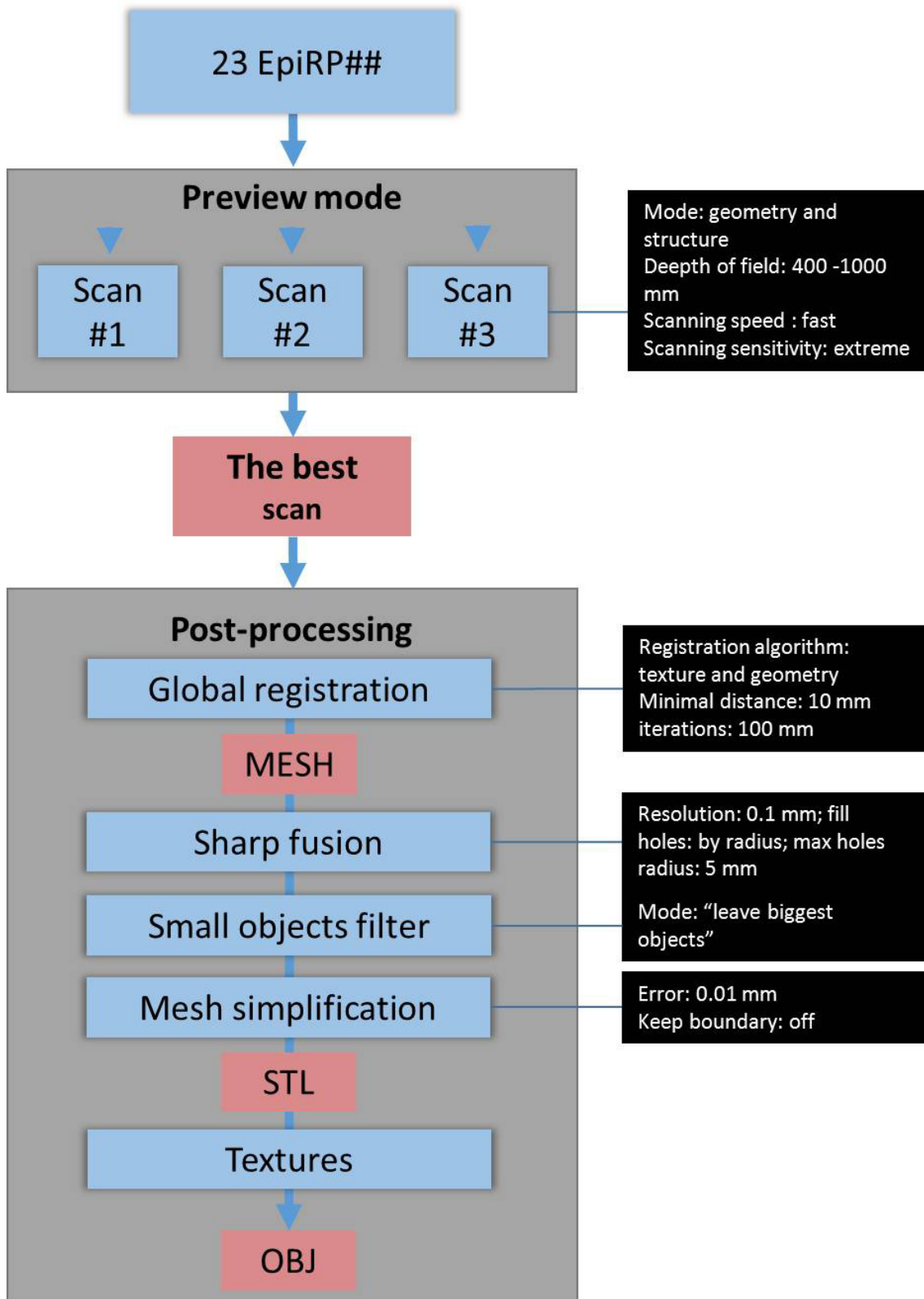


**Figure 9. Post-processing chain** including the settings for each of the 23 enrolled EpiRP cases to obtain images in OBJ format

### 2.3.3 Distance measurements in the CAD software

Section measurements (see Table 2/distances on page 26) were evaluated with the tool “digital lineal” (Artec Studio, Artec Group) (Figure 10 on page **Fehler! Textmarke nicht definiert.**). All distances were measured three times. As the distance was continuously displayed on the measurement line, the operator concentrated on the landmarks without noticing the displayed value.

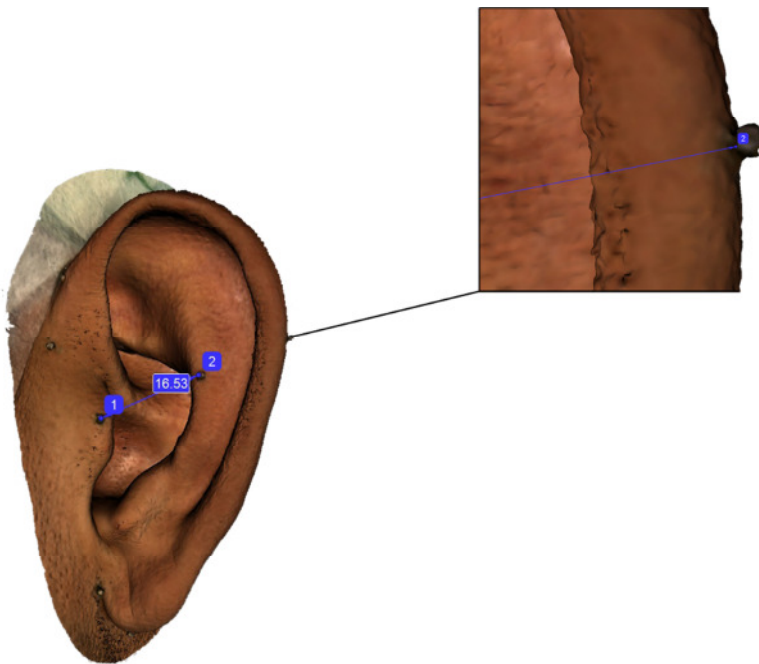


**Figure 10** Distance measurement in the CAD software with the "digital lineal" tool

### 2.3.4 CAD Modelling

This step implied the surface inspection to reveal, if the models were “waterproof” and ready for the further additive manufacturing process. Each 3D model was provided with a basis at the temporal site to make it possible to stand on a plain surface (Figure 11, see below).



**Figure 11.** 3D model of the ear APR after being edited in the CAD-software and ready for the further AM-process

### 2.3.5 Additive manufacturing

Gathered digital files in OBJ format were used to produce the APRs by means of the AM methods: SLS, FDM, and SL (Figure 12 – see below; Table 3 on page 33). Due to the limited financial budget of the study and because producing SL patterns is so costly the AM production of ARPs with this method was limited to the first 11 EpiRP cases.



**Figure 12.** APRs manufactured respectively with SLS, SL, and FDM methods



AM methods	Production description					
	Firm	AM machine	Production time	Production cost	Material used	Layer thickness
<b>SLS</b>	Jomatik GmbH (Tübingen, Germany)	SPro 60 HD (3D Systems, Rock Hill, USA)	11 hours	65 Euros	Polyamide powder	0.08 mm
<b>FDM</b>	Rioprinto (Stuttgart, Germany)	The Makerbot 2 (MakerBot Industries, New York, USA)	3 hours 27 minutes	25 Euros	PLA	0.1 mm
<b>SL</b>	3D-Store (Moscow, Russian Federation)	ProJet SD 7000 (3D Systems, Rock Hill, USA)	16 hours	120 Euros	Polycarbonate	0.025 mm

Table 3. Features of AM methods utilization

## 2.4 Quantitative Analysis of dimensional accuracy

### 2.4.1 Definition of data sets and data groups

Each participant forms a data set, containing five following data groups.

**“in vivo”**: values of the analogue measurements from the participants natural ears:  
→ “reference measurement”

**“CAD”**: values of the digital measurements from the CAD software (Artec Studio, Artec Group).

**“SLS”, “FDM”, and “SL”**: values of the measurements from the APRs, produced respectively with SLS, FDM, and SL methods:  
→ “replica measurement”.

- The “in vivo” measurement served as first reference (gold standard) for comparison with the subsequent measurements from CAD and APRs. Comparison between those two measurements represented the accuracy of the whole digital work flow starting from the scanning process and ending in the manufacturing of an auricular prosthesis replica.
- The “CAD” measurements were used as the second reference for comparison with measurements from APRs. Thus, they represented the accuracy of the different AM methods used in this study to manufacture an auricular prosthesis replica.
- Each data group consists of seven distances. Each distance was repeatedly measured three times.

### 2.4.2 Preparing the Datasets

All measured values were written down into a table of the statistical package JMP (Version 11.1, SAS Institute Inc., Cary, NC, USA).

A dataset is qualified by the pseudonym number *EpiRP-##* as “ID” of the participant followed by the measurements (groups, sections).

Data entry was cross checked for plausibility and missing data by distributions as described by Altman [2].

#### 2.4.3 Calculation of the measurement error

The measurement error of each sections of measurement is calculated for each data group. Therefore the measurements in each data group are calculated according to Bland and Altman – [8]. Repeatability can be determined by multiplying the measurement error (ME) with 2.77 ( $=1.96*\sqrt{2}$ ) and interpreted as follows [8]. The difference between two measurements under same conditions, here measurements of a specific section of a specific data group, is at least  $ME*2.77$ . This assertion, however, will be expected for 95 % of pairs of measurements for each section of measurement within each data group. Using 0.3 mm as an upper bound of ME in the situation described in this article, repeatability is computed as 0.8 mm. This is found to be clinically acceptable for the detection of 1.5 % or 2 mm deviation.

#### 2.4.4 Comparing data groups

The data groups are compared using the approach of differences in matched pairs and mean of means, known as Bland-Altman-Plot [9].

Additionally relative differences between the data groups are calculated using the following formula [62, 74]:

$$\frac{\text{replica measurement} - \text{reference measurement}}{\text{reference measurement}} \times 100$$

## 2.5 Qualitative analysis of skin texture reproduction

To investigate the skin texture reproduction of APRs manufactured respectively with SL, SLS, FDM a gold standard is needed. This was found in a “classic” gypsum cast made from a conventional silicon impression. This impression was made additionally to all other study measures from participant #17, using an addition-curing silicone (Multisil Epithetik, Bredent, Neu-Ulm, Germany). The stone cast was poured with dental stone class IV (VelMix Stone, Kavo-Kerr, Rastatt, Germany).



**Figure 13. Stone cast of one of the probands to measure the surface roughness**

### 2.5.1 Reference areas for analysis

Several reference areas on the stone cast have been defined – “Helix” and “Lobula”. These areas were used for the analysis with a stereomicroscope. Additionally, two biggest skin wrinkles, which were easily recognized – “Lobula basis” and “Lobula corpus”, and also one wrinkle called “Helix” have been set as a minimum level of skin texture reproduction for the AM methods in combination with a structured light scanner (Figure 14 on page 37).

### 2.5.2 Stereomicroscopy

The areas “Helix” and “Lobula” were thoroughly examined with the use of stereomicroscope (WILD 400, Heebrugg, Switzerland). Four photographs of each APR and the gypsum model with tenfold and sixteen fold enlargement have been taken and afterwards compared visually to each other. It was referred to the initial CAD image that all the AM machines have used in order to check, on which production stage the deviations from the original anatomy occur.

### 2.5.3 Profilometry

Profilometry was used to measure the roughness of the skin texture, which can be reproduced by the different AM methods compared to the gypsum replica. (Perthometer S6P, Mahr, Göttingen, Germany). A little stand was made from silicone material to ensure the same position of each of the 3 APRs. Each wrinkle of “Helix”, “Lobula basis” and “Lobula corpus” on each APR and referent stone cast was analysed (Figure 14 – see below). Four single profiles for each wrinkle across 3 mm distance were recorded. The profile depth (Pt parameter) was measured with the special software (MountainsMap Digital Surf). The mean profile depth was calculated for each wrinkle.

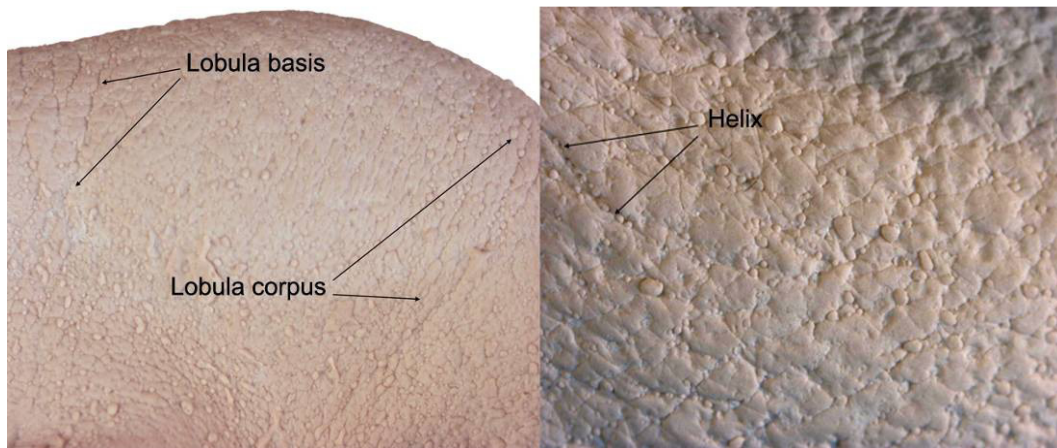


**Figure 14. Location of the wrinkles to be examined with the use of profilometry**

### 3 RESULTS

#### 3.1 Participants and measurements

##### 3.1.1 *Missing measurements*

The short distances (sa-sa', pa-pa' and sba-sba') turned out to be measured with difficulties, as some areas posterior to the auricle were unattainable for the digital calliper (Figure 3 on page 24 and Table 1 on page 25). Moreover landmarks, such as "sba", didn't have any bony or cartilaginous support. Others (sa', pa') were located in the haired area which needed to be covered by the cap. This provided the landmarks with a certain degree of pliability, especially sa', which reduced reproducibility in vivo.

In five datasets the sa-sa' distance was unfeasible to be measured at all and was neglected in the further analysis. In other cases the measurement of all short distances showed the poor repeatability might have been error-prone.

For this reason the mean relative difference between the groups of measurements has been calculated in two ways: first, using all distances and second, neglecting the "short distances" (sa-sa'; pa-pa'; sba-sba').

The surface structure analysis yielded, that the wrinkle "Helix" was not able to be reproduced on AM-manufactured APRs. For this reason the profilometry of this wrinkle was unfeasible.

### 3.1.2 Calculation of measurement error

Table 4 (see below) shows the number of measurements and measurement error (ME) of the single measurements derived from 23 in vivo, CAD, SLS, FDM APRs as well as 11 SL APRs.

Measurement sections	Data groups of measurements				
	IN VIVO	CAD	SLS	FDM	SL
sa-sba	n=69	n=69	n=69	n=69	n=33
	66.52; 6.52	66.84; 6.71	67.08; 6.71	66.68; 6.66	64.93; 6.06
	0.253	0.228	0.178	0.351	0.2
obs-obi	n=68	n=69	n=69	n=69	n=33
	46.41; 5.73	46.56; 5.67	46.75; 5.63	46.61; 5.7	45.82; 6.48
	0.328	0.155	0.295	0.230	0.277
pa-pra	n=69	n=69	n=69	n=69	n=33
	40.1; 4.01	40.31; 4.09	40.17; 4.1	40.15; 4.1	38.46; 3.16
	0.274	0.164	0.295	0.206	0.164
tra-ah	n=69	n=69	n=69	n=69	n=33
	23.83; 3.14	23.64; 3.15	23.74; 3.17	23.62; 3.17	22.42; 4.0
	0.236	0.210	0.184	0.260	0.211
sa-sa'	n=50	n=52	n=51	n=54	n=18
	10.74; 3.96	10.89; 4.11	11.2; 4.02	11.14; 4.04	9.02; 2.94
	0.366	0.143	0.180	0.171	0.145
pa-pa'	n=67	n=69	n=69	n=68	n=32
	18.41; 4.45	18.63; 4.48	18.75; 4.52	18.75; 4.45	18.43; 5.31
	0.262	0.250	0.248	0.189	0.161
sba-sba'	n=67	n=69	n=60	n=60	n=27
	12.56; 4.59	12.3; 4.76	12.18; 4.53	12.21; 4.55	12.91; 5.71
	0.256	0.285	0.247	0.265	0.210
<b>Mean of ME</b>	<b>0.282</b>	<b>0.205</b>	<b>0.232</b>	<b>0.239</b>	<b>0.195</b>

**Table 4. Measurement error (ME) within the data groups.** The cells contain the number (n, first row) of measurements available within one data group for each section of measurement. The second row in each cell shows the calculated value of mean measurements and the SD. The third row contains the measurement error of the single measurements. The last row of the table contains the mean value of the measurement error within the data group.

The MEs were comparable across all data groups. Thus, the single measurements were averaged by the arithmetic mean for further calculations of the mean differences.

### 3.1.3 Mean differences towards the reference

Table 5 (see below) contains the mean differences between in vivo, CAD, FDM, SLS and SLS data groups, gathered respectively from participants, CAD software, APRs produced by FDM, SLS and SL.

Data groups	Measurement sections (mm)						
	Short distances			Medium distances		Long distances	
	sa-sa' <i>d</i>	pa-pa' <i>e</i>	sba-sba' <i>f</i>	pa-pra <i>b</i>	tra-ah <i>g</i>	sa-sba <i>a</i>	obs-obi <i>c</i>
<b>In-vivo/ CAD</b>	n=18 <b>0.15</b> (-0.12, 0.43)	n=23 <b>0.22</b> (-0.05, -0.5)	n=23 <b>-0.29</b> (-0.54, -0.03)	n=23 <b>0.21</b> (0.7, 0.35)	n=23 <b>-0.19</b> (-0.36, -0.02)	n=23 <b>0.32</b> (0.07, 0.57)	n=23 <b>0.15</b> (-0.12, 0.43)
<b>In-vivo/ FDM</b>	n=17 <b>0.07</b> (-0.22, 0.35)	n=23 <b>0.34</b> (0.02, 0.67)	n=21 <b>-0.18</b> (-0.51, 0.14)	n=23 <b>0.06</b> (-0.14, 0.25)	n=23 <b>-0.21</b> (-0.45, 0.03)	n=23 <b>0.16</b> (-0.14, 0.45)	n=23 <b>0.20</b> (-0.08, 0.49)
<b>In-vivo/ SLS</b>	n=17 <b>0.12</b> (-0.17, 0.42)	n=23 <b>0.34</b> (0.05, 0.63)	n=21 <b>-0.21</b> (-0.53, 0.12)	n=23 <b>0.07</b> (-0.06, 0.21)	n=23 <b>-0.09</b> (-0.3, -0.11)	n=23 <b>0.56</b> (0.28, 0.84)	n=23 <b>0.35</b> (0.07, 0.62)
<b>In-vivo/ SL</b>	n=6 <b>-0.06</b> (-0.68, 0.57)	n=11 <b>-0.02</b> (-0.45, 0.41)	n=10 <b>-0.22</b> (-0.85, 0.41)	n=11 <b>0.18</b> (-0.08, 0.44)	n=11 <b>0.07</b> (-0.24, 0.38)	n=11 <b>0.32</b> (-0.04, 0.68)	n=11 <b>0.48</b> (0.16, 0.81)
<b>CAD/ FDM</b>	n=17 <b>-0.05</b> (-0.16, 0.06)	n=23 <b>0.12</b> (-0.004, 0.25)	n=21 <b>0.07</b> (-0.07, 0.20)	n=23 <b>-0.15</b> (-0.29, -0.02)	n=23 <b>-0.02</b> (-0.15, 0.11)	n=23 <b>0.16</b> (-0.28, -0.05)	n=23 <b>0.05</b> (-0.09, 0.18)
<b>CAD/ SLS</b>	n=17 <b>0.01</b> (-0.11, 0.13)	n=23 <b>0.12</b> (0.03, 0.21)	n=21 <b>0.04</b> (-0.09, 0.17)	n=23 <b>-0.14</b> (-0.24, -0.03)	n=23 <b>0.10</b> (0.01, 0.18)	n=23 <b>0.24</b> (0.17, 0.31)	n=23 <b>0.19</b> (0.06, 0.32)
<b>CAD/ SL</b>	n=6 <b>-0.03</b> (-0.23, 0.16)	n=11 <b>0.04</b> (-0.06, 0.15)	n=10 <b>0.22</b> (0.10, 0.33)	n=11 <b>-0.09</b> (-0.26, 0.07)	n=11 <b>0.07</b> (-0.08, 0.22)	n=11 <b>0.20</b> (0.08, 0.32)	n=11 <b>0.27</b> (0.12, 0.42)

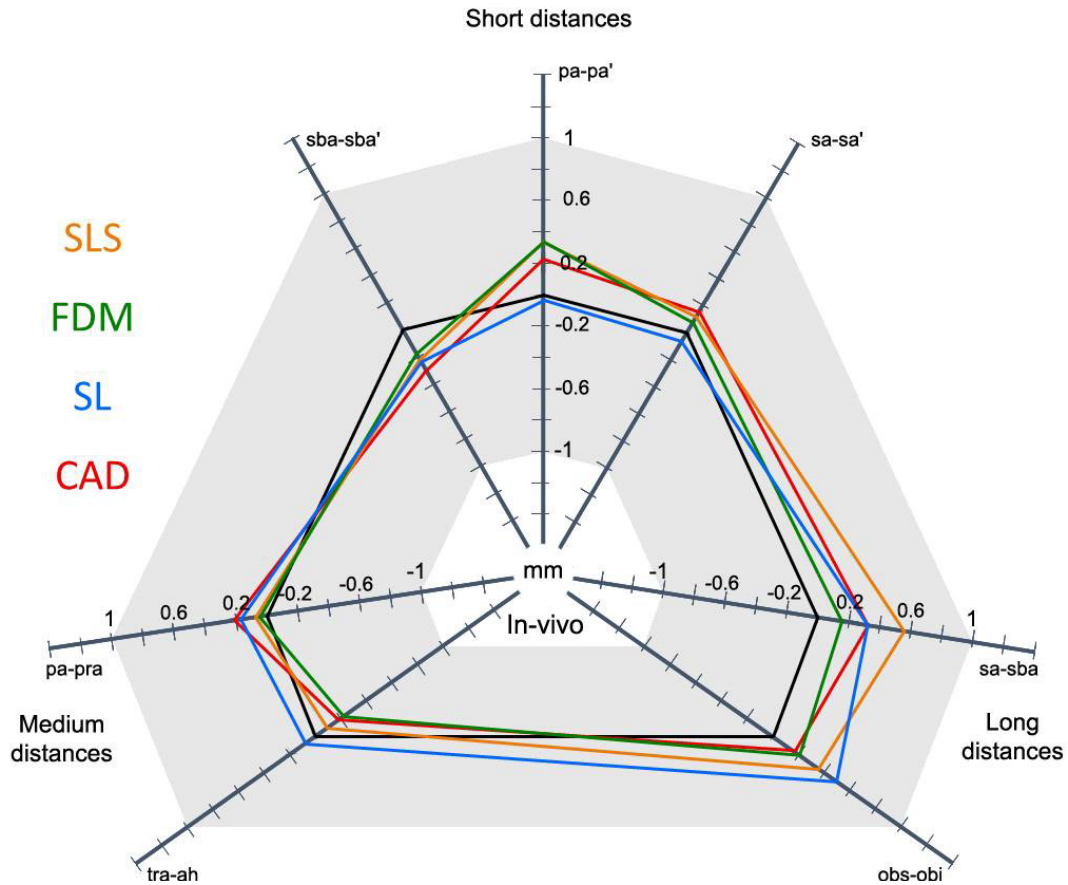
**Table 5. Mean differences (Biases) of in vivo and CAD measurements compared towards measurements on the 23 SLS, 23 FDM, and 11 SL APRs.** A cell contains the number of mean measurements (n), the mean difference towards the CAD measurement followed by the minimum and maximum value of bias.



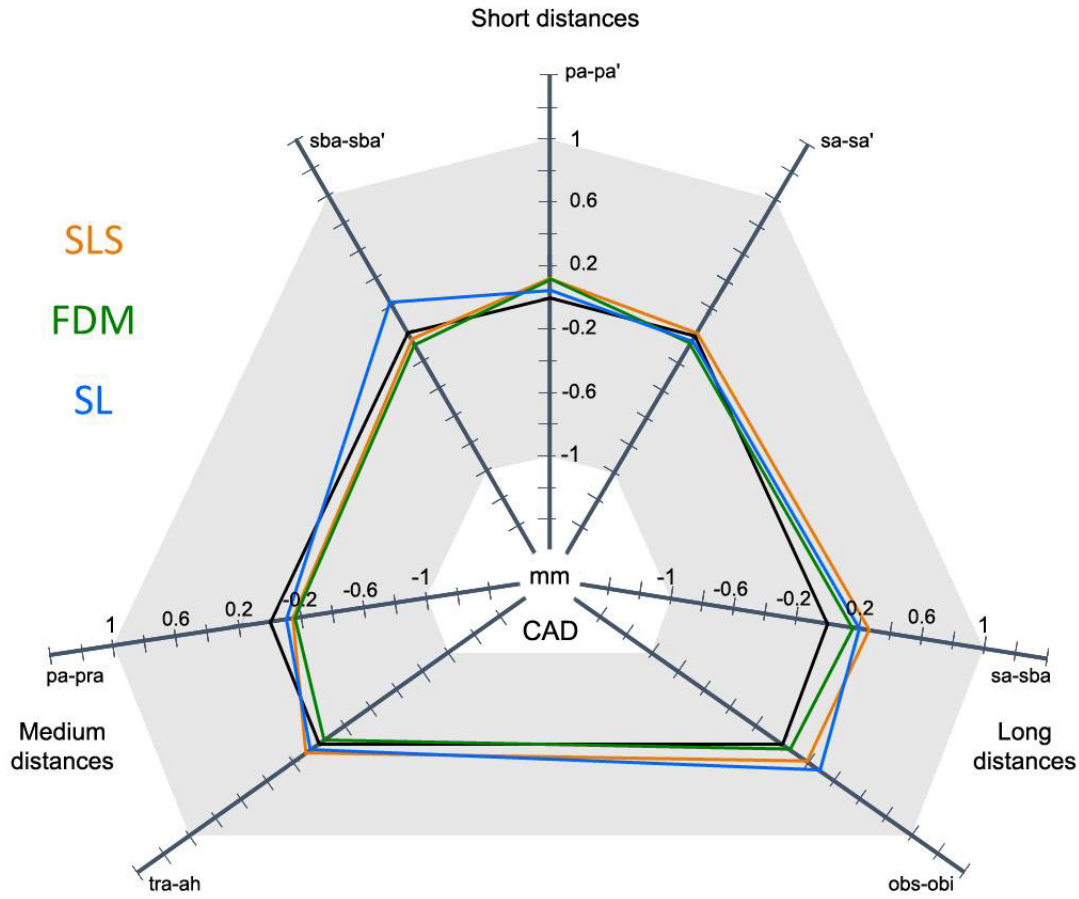
Measurements of the SL or especially FDM APRs showed the smallest deviations from the respective ones in vivo. The lowest biases were identified four times in FDM (sba-sba', pa-pra, sa-sba, obs-obi), three times in SL-APRs (sa-sa', pa-pa' and tra-ah), and not once in SLS.

The graphic below depicts the overall situation (Figure 15). On this graphic the colored lines represent each AM method. The black solid line represents the absolute zero (in vivo measurements). The grey field represents the threshold of the clinical relevance, which is 1 mm in each direction from the zero line (in sum 2 mm) [25]. According to the way, how the other lines relate to each other and how far they are situated to the zero-line (black), the ratio between the mean differences of in vivo measurements to each AM-method can be ascertained. It can be clearly seen, that none of the lines exceed the grey field of optical clinical relevance. Still, the green line, representing the FDM method is placed closer to the absolute zero in most sides of the graphic. Thus, it can be assumed, that the methods of FDM showed a superior dimensional accuracy, than others.

Data in the table 5 (page 42) indicates that measurements performed on SLS and SL models had two times the smallest bias towards the CAD reference. In contrast, FDM-produced models had three times the lowest difference to the CAD reference. On Figure 16 (page 43) it can be seen that the green line representing the FDM method lies closer to the black one (on this graphic – CAD reference), than the others. Thus, the FDM can be regarded as the best towards dimensional accuracy.



**Figure 15. Mean absolute differences (Bland and Altman plot) of in vivo measurements compared towards measurements of 23 SLS, 23 FDM and 11 SL APRs and towards CAD measurements.** Each colour of the line represents respectively the groups of measurements listed in table 5 on page 40. The shaded area around the black reference line (0) indicated the 2 mm deviation of clinical relevance.



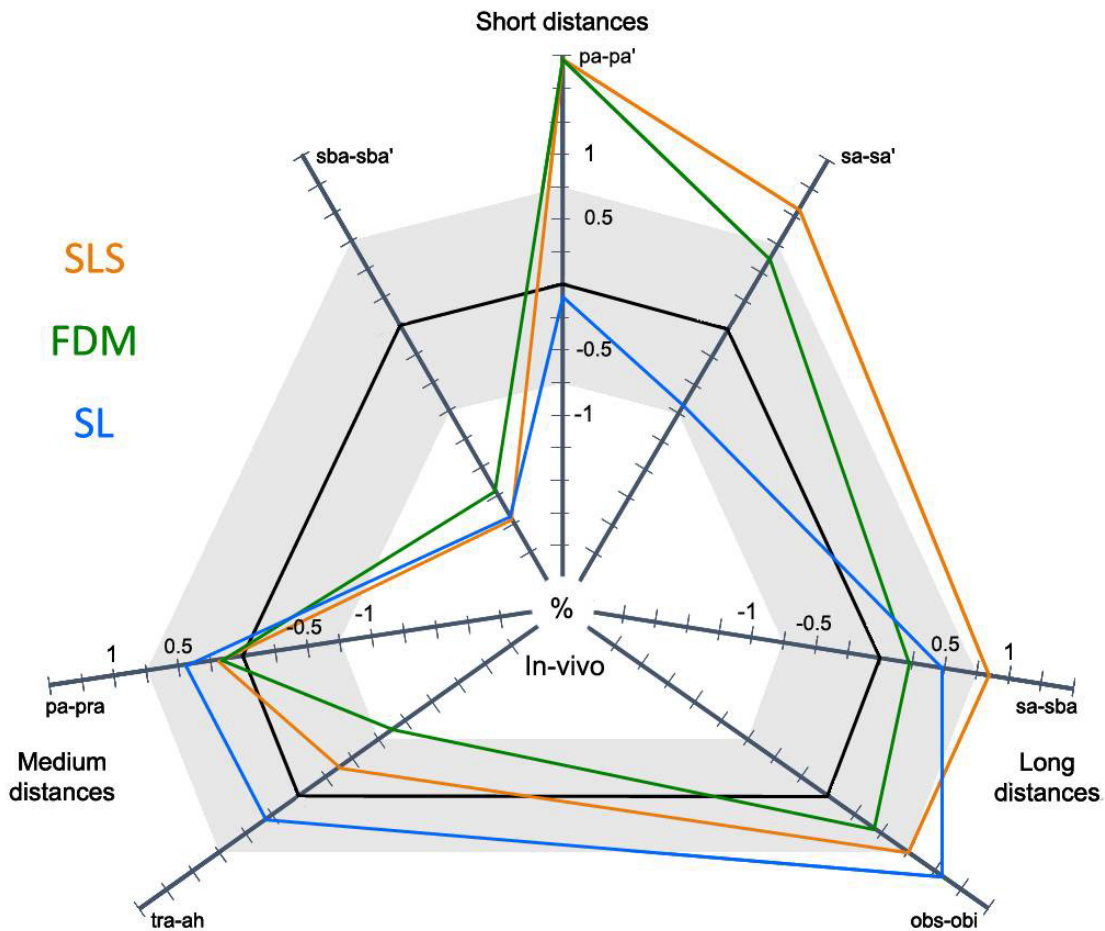
**Figure 16. Mean absolute differences (Bland and Altman plot) of CAD measurements compared towards measurements of 23 SLS, 23 FDM and 11 SL APRs.** Each colour of the line represents respectively the groups of measurements listed in table 6. The shaded area around the black reference line (0) indicated the 2 mm. deviation of clinical relevance.

Table 6 (see below) shows the relative differences between the in vivo and CAD groups towards measurements made for each group of AM methods.

Initially, the best method compared to in vivo measurements was SL; compared to CAD data group – FDM. When short distances were neglected, as they were considered to initiate the most of discrepancies between the groups of measurement, the FDM method showed the best accuracy compared to both in vivo and CAD data groups (Figure 17 on page 45, Figure 18 on page 46).

Measures	Mean relative differences between AM methods used (%)					
	SLS		FDM		SL	
	In vivo	CAD	In vivo	CAD	In vivo	CAD
sa-sba	0.84	0.36	0.24	-0.24	0.49	0.31
obs-obi	0.75	0.41	0.43	0.11	1.07	0.59
pa-pra	0.17	-0.35	0.15	-0.37	0.47	-0.23
tra-ah	-0.38	0.42	-0.88	-0.08	0.31	0.31
sa-sa'	1.08	0.09	0.63	-0.45	-0.67	-0.33
pa-pa'	1.84	0.64	1.85	0.64	-0.11	0.22
sba-sba'	-1.69	0.33	-1.46	0.57	-1.68	1.73
Total mean (all)	0.96	0.37	0.81	0.35	0.69	0.53
Total mean (w/o short distances)	0.54	0.39	0.43	0.20	0.59	0.36

**Table 6. Mean relative differences of AM methods compared to in vivo and CAD measurements.** The highest values are marked with the red colour, the lowest with – green. Total mean is calculated with (all) and without (w/o) short distances due to the measurement bias/missing values of short distances.



**Figure 17. Mean relative differences (Bland and Altman plot) of in vivo measurements compared towards measurements of 23 SLS, 23 FDM and 11 SL APRs.** Each colour of the line represents respectively the groups of measurements. The shaded area around the black reference line (0) indicated the 1.5% deviation of statistical relevance.

The comparative analysis showed that the hypothesis  $i$  can be accepted (see page 19). The comparison of the absolute mean differences of AM replicas to in vivo did not reveal any clinically relevant deviation exceeding 2 mm. However, the analysis of *relative* mean differences detected discrepancies up to 1.85 %.

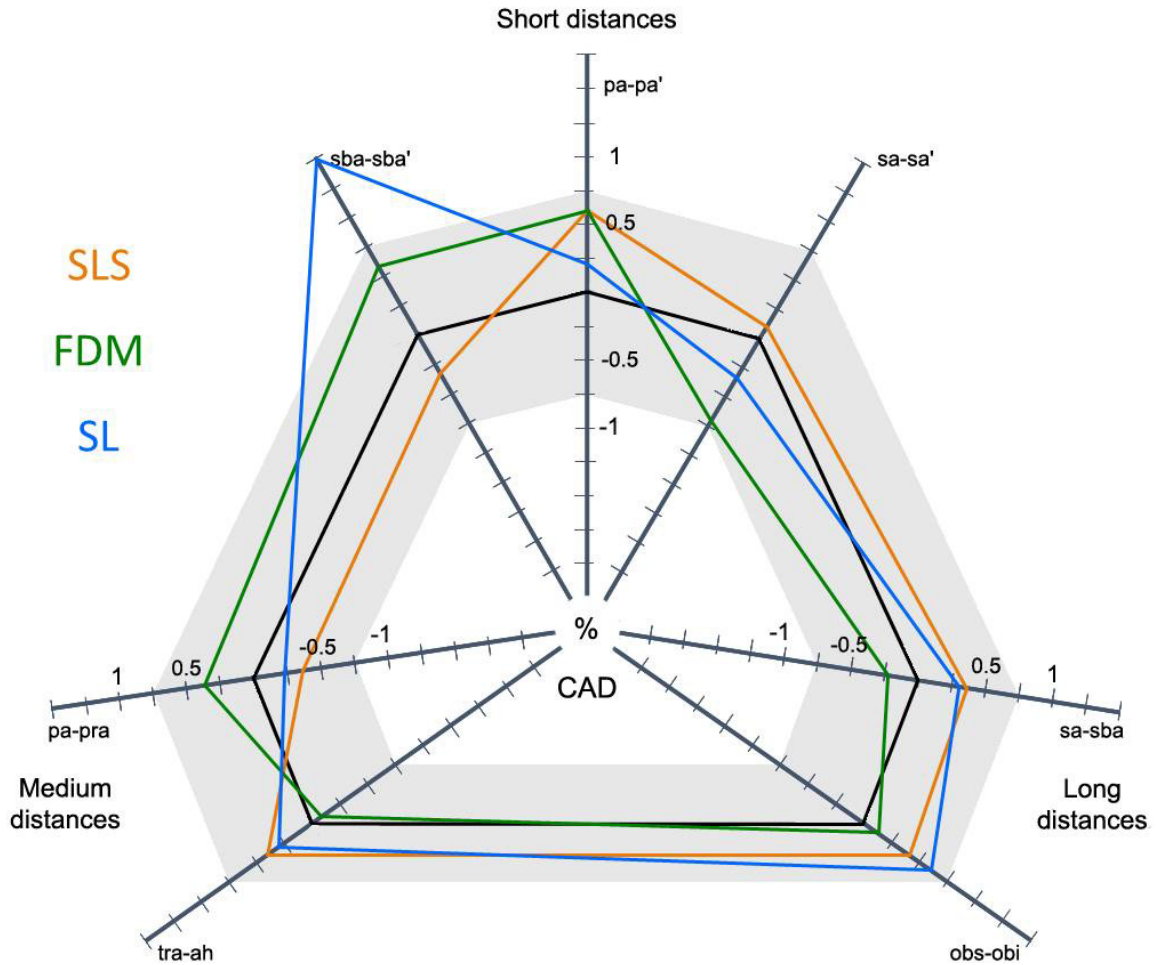


**Figure 18.** Mean relative differences (Bland and Altman plot) of in vivo measurements compared towards measurements of 23 SLS, 23 FDM and 11 SL APRs. Each colour of the line represents respectively the groups of measurements. The shaded area around the black reference line (0) indicated the 1.5 % deviation of statistical relevance

The comparative analysis showed the hypothesis *ii* can be accepted. The comparison of the absolute mean differences of AM replicas to CAD did not reveal any clinically relevant deviation. The analysis of *relative* mean differences detected a deviation from the in vivo data group in only one case of SL, which exceeded the threshold of clinical relevance.

## 3.2 Skin surface analysis

### 3.2.1 *Visual analysis of the surface*

The visual comparison of the stereomicroscopic pictures revealed that none of the AM methods used in combination with a structured light scanner was able to reproduce truly the skin structure. The wrinkle “Helix” was completely missing on each APR (see page 36). The wrinkles “Lobula basis” and “Lobula corpus” could be reproduced, using a digital approach of prostheses manufacturing on each APR (Figure 20 – see below). With regards to the surface structure it must be said that it deviated considerably from the original anatomy (gypsum model). Thus, the texture of the FDM-produced APR was comprised of PLA filaments, which were still recognizable even after the layers were solidified with each other. The surface of the SLS-produced model was mostly comprised of the little powder particles and has also failed to describe the original surface structure. The APR made by means of SL showed a very smooth surface with absolute absence of staircase effect. However, all the skin structure details were completely missing.

It must be also stressed that on each APR the wrinkles “Lobula basis” and “Lobula corpus” were even more pronounced (compared visually), than on the stone cast.

The “Helix” wrinkle could not be described on any of APRs (Figure 19 – see below). The examination of the three-dimensional image (Figure 21 on page 49) disclosed that the “Helix” wrinkle has not been longer displayed yet in the CAD software. Compared to the 3D image of the “Helix” area, the FDM-produced APR showed the best resemblance, followed by SLS-produced APRs (compared visually).



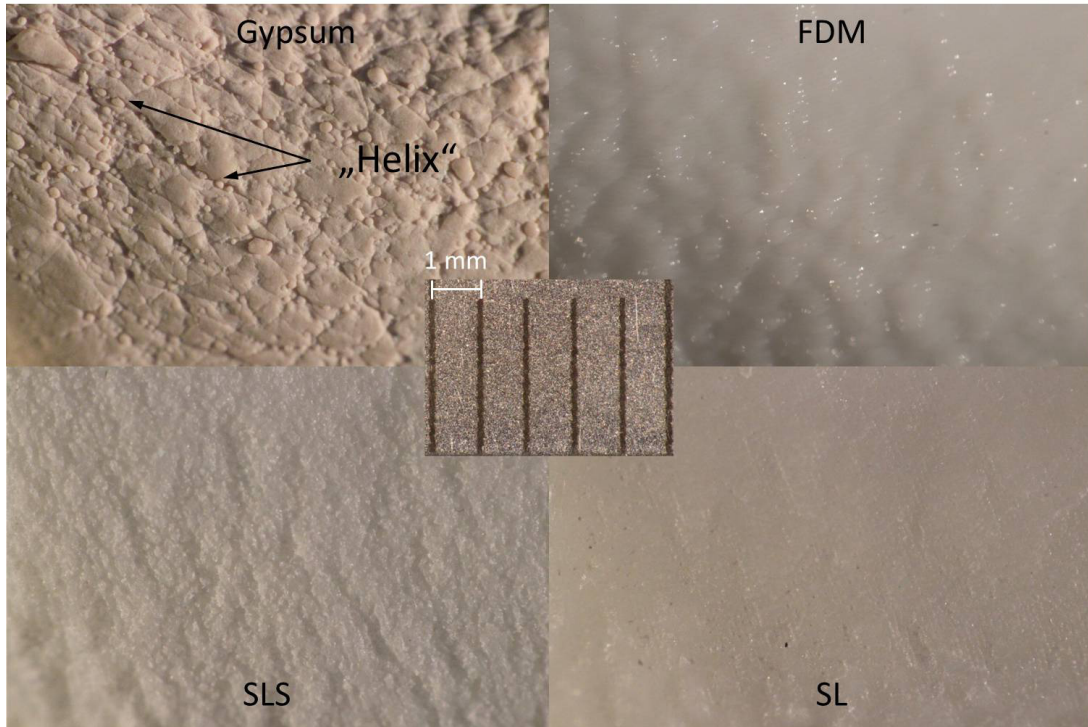


Figure 19. Stereomicroscopy of three FDM-, SLS-, SL-produced APRs and one stone cast with the 16x enlargement

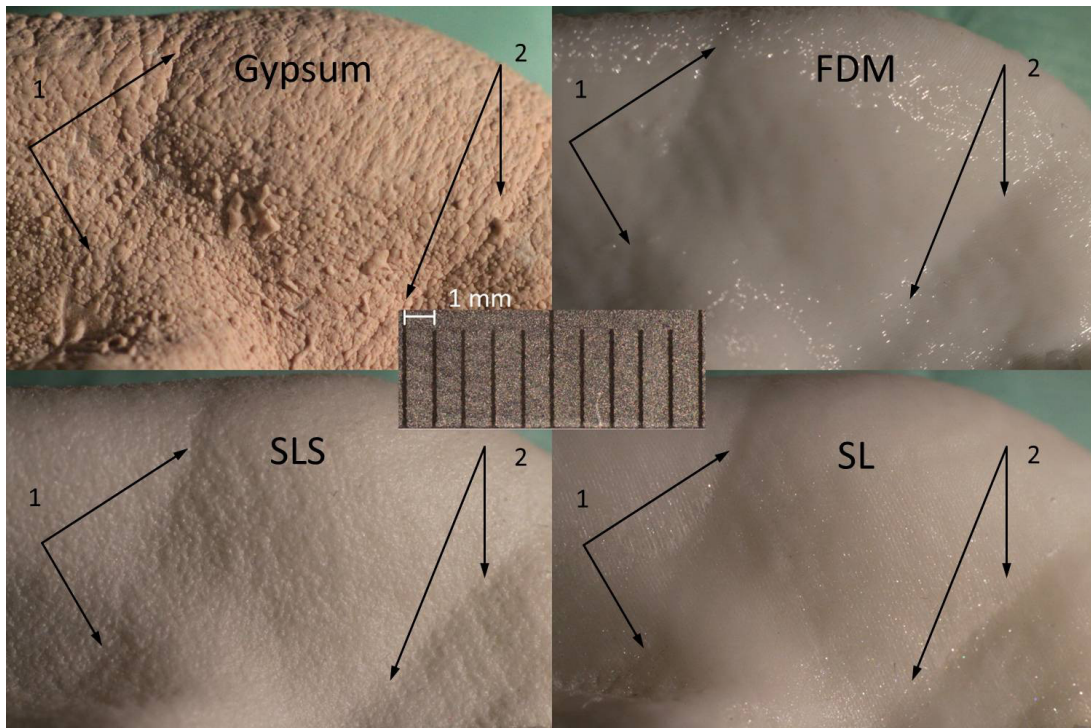
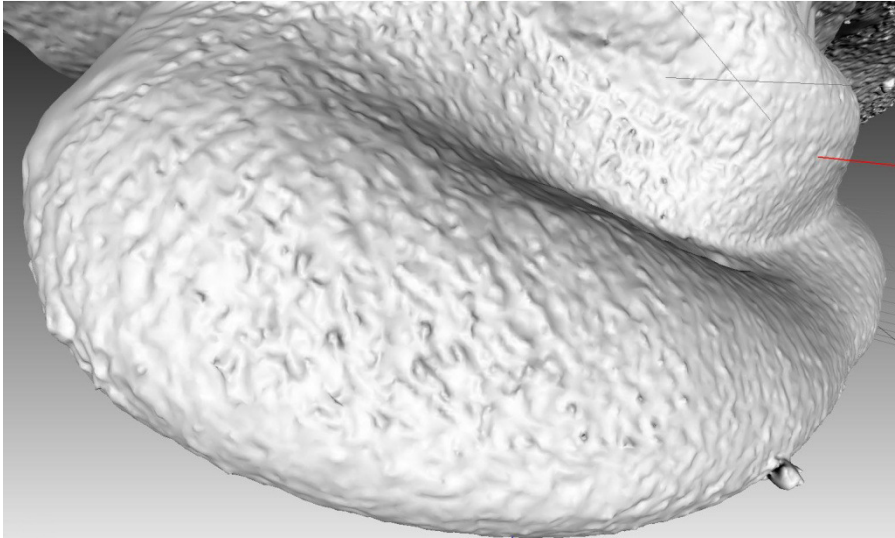


Figure 20. Stereomicroscopy of three FDM-, SLS-, SL-produced APRs and one stone cast in "Lobula" area with the 10x enlargement. 1- "Lobula basis"; 2 - "Lobula corpus".





**Figure 21 “Helix” area on the three-dimensional image, AM methods have addressed to. The wrinkle "Helix" is not captured.**

### 3.2.2 Profilometry

The Table 7 represents the mean value of each wrinkle depth. The profilometrical analysis of the “Helix” wrinkle was neglected, as it was not recognizable on any of APRs.

APR	Wrinkles location and their Pt ( $\mu\text{m}$ )		
	Helix	Lobula basis	Lobula corpus
Gypsum	94	192	220
SLS	-	235	265
FDM	-	209	229
SL	-	156	214

**Table 7. Mean (Pt) values of the reference wrinkles**

The average depth of the “Helix” wrinkle on the reference gypsum model was  $94 \mu$ . It has failed to be reproduced by means of digital approach used in the study. The “Lobula basis” wrinkle on the reference gypsum model was  $192 \mu$  deep, which let it to be recognized and captured fully by a structured light scanner. The same was with the “Lobula corpus” with its depth of  $220 \mu$ .

The following graphic (Figure 22 – see below) additionally provided for “Lobula basis” wrinkle displays the differences in the wrinkles geometry. The profile of FDM-produced APR is comprised of the wave-like line, which represents the PLA filaments. This wave-effect impairs the overall semblance of the APR surface. The profile line of APR made by SLS is quite similar to the stone model, but still deviates from it. As far as the surface of SL-made APR was slightly smoothed, the depth on the wrinkle was as well reduced and profile line appeared to be relatively straight. Thus, none of the AM methods was able to reproduce the skin surface texture entirely.

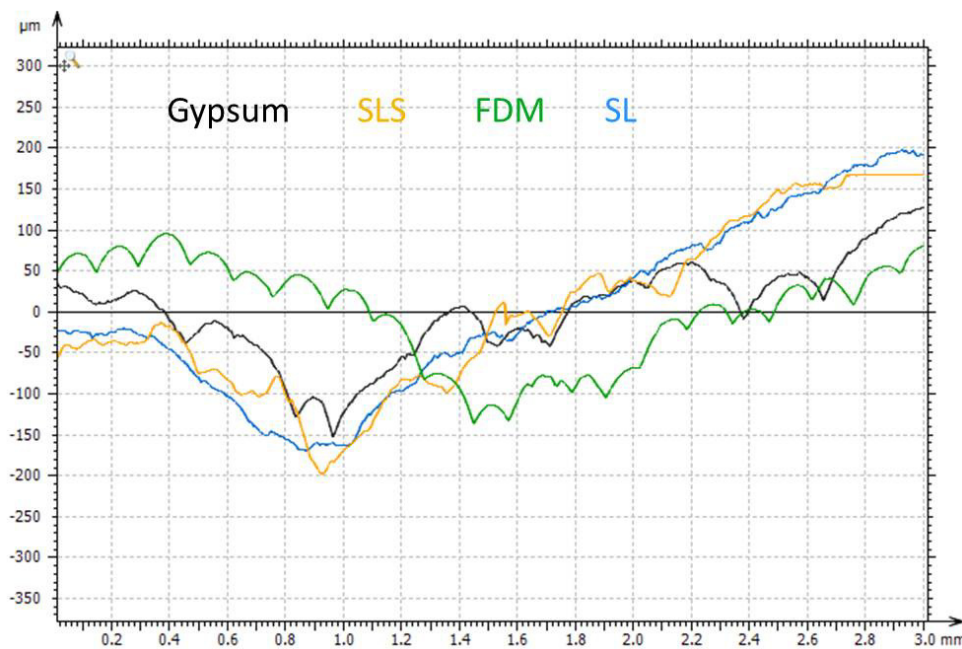


**Figure 22. Profile graphics of the three "Lobula basis" wrinkle of gypsum model (black line), SLS-produced APR (orange line), FDM-produced APR (green line) and SL-produced APR (blue line). None of the lines is similar to the referent black one.**

All the results contradict the hypothesis number *iii*. The assumed statement that the surface structured light scanner in combination with the AM-methods used in this study enables to reproduce the skin surface texture with the detailing level of 0,1 mm was disproved. Only partial reproduction might be feasible, where the skin details exceed 192 µm of depth.

### 3.3 Production costs and time

Each APR manufactured by means of SLS has cost about 65 Euros. The average production time was 16 hours. The production of 11 APRs by means of SL method lasted 11 hours and has cost 120 Euro pro each APR. It was not possible to calculate the production time for each APR, as they were made simultaneously. In case of FDM each APR costs 25 Euros and the production time per one case was 2-3 hours.

Comparing the outcomes according to the last question (hypothesis *iv*) FDM was identified at this point of time as the “best-in-practice” method.

## 4 DISCUSSION

### 4.1 Discussion of applied methods

#### 4.1.1 *Probands and recruiting*

For this study the RP approach was chosen, as the literature analysis revealed that it has been frequently used, but only as case reports [82, 84, 88]. Far no study aimed a systematic analysis of the accuracy of the digital work flow in reproducing an artificial ear.

In order to investigate the accuracy of AM methods employed for fabrication of APRs, it is not obligatory to perform the scans on real patients suffering from a kind of facial disfigurement. Enrolment of healthy subjects, having their both ears present was beneficial in terms of easier carry out of the study. It has not afflicted negatively the objectiveness of the study in terms of proper application of the selected approach (RP - indirect mold making). The current trial replicated the same ear, which was scanned. This allows a direct compatibility of the acquired data between in vivo and the derived data groups of CAD and AM.

The cohort is aged in mean 37.8 years. Subjects under the 18 y.o. might be impatient and not able to stay still for a long period, while performing the anthropometry and scanning.

#### 4.1.2 *Data acquisition/ scanning of ears/ digitalisation*

Digital capturing of the whole ear anatomy may be challenging due to the big number of undercuts.

Some other authors have utilized the approach, where the traditional impression of the auricle is first taken [1, 20, 45]. The obtained stone cast is later on scanned with a stationary laser scanner, such as 3Shape R700 (3Shape, Denmark) [84]. This kind of

stationary scanners is cheaper to work with. However, the additional step of impression taking makes the study measures error-prone.

The use of medical imaging systems such as CT and MRI allows to capture the whole ear anatomy with its numerous undercuts. However, it can be very difficult to justify performing of a CT scan just for scientific purposes without any clinical need.

For this reason we used the structured light scanning (Artec Spider Scanner). This system allowed to capture the complete ear anatomy within a reasonable time, as it is handheld and thereby allowed to perform the scanning from different angles in order to attain the areas, that were obscured from the line of sight.

In the studies to the topic some other scanners have been employed. A stationary laser scanner (Desktop 3D Scanner; NextEngine, Santa Monica, USA), for instance, was used by Ciocca [17, 21]. The fact, that the scanner must remain still significantly compromises the overall quality of the obtained images and from our point of view would not be applicable in our study.

Comparable portable systems, such as Breuckmann Opto TOP-HE [33, 79] and Polhemus FastScan [11] have been used in the mentioned studies. The scanning accuracy of these systems was reported to be 45  $\mu$  and 18  $\mu$  respectively, which is comparable to the system we have used in the study with its accuracy in the order of 50  $\mu$ . It has been reported in the study of Cheah (2003) that the scanning accuracy up to 0.5 mm is sufficient for facial prostheses manufacturing [13]. Thus, the resolution of the scanner used in the present study was assumed to be also sufficient.

#### *4.1.3 Measurements and measurement error*

The major concern of the scientific researches was always to find out whereupon the persisting errors of AM process depend [49, 74]. Data acquisition process and the reliability of the measurements are recognized as the main limiting factors, when investigating the dimensional accuracy of AM methods [24, 25, 74, 86].

Some landmarks are commonly not easy to be located and recognized on different stages of the study. Such discrepant identification of the landmarks impairs

considerably the repeatability of the measurements [36]. It may be overcome by using the fiducial markers [40, 87]. In the present study each landmark was previously pointed out on the ear surface with accordance to the anthropometrical protocol chosen and provided with volume, so that they were recognizable on other stages throughout the study.

Distortions may be also caused due to a contact of a measuring instrument to the soft tissues [36]. The pressure that is caused by each measurement cannot be monitored and equilibrated. As far as all tissues are differently pliable, mostly those of them that do not have any bony support, fiducial landmarks are occasionally shifting. The measurement values are this way error-prone. That's why in the present study the measuring process follows the recommendations for metrology [10]. The measurement error within all groups of measurements was calculated between 0.20 mm and 0.29 mm (see Table 4 on page 39). Thus, the measurement errors are comparable and not dependent on a model. This implies a high reproducibility of the measurements.

The objectivity of dimensional accuracy investigation may also correspond to a study design. Most of the common researches establish ideal conditions, where the reference object is fixed and unanimated, as being just a model [62, 73, 78]. This way any movements and tissue pull would not be apparent. Such conditions vary extremely from those that we have in a daily medical practice, as patients do produce slight mimic motions such as blinking or corrugating the forehead. For this reason we performed our study on the healthy subjects.

#### *4.1.4 Manufacturing methods*

The literature analysis revealed that the AM methods used in this study, namely SLS, SL and FDM were most frequently used in other clinical case studies and scientific researches on the topic of maxillofacial prosthetics [21, 39, 60, 63, 73]. The only exception in those terms was the method of 3D-printing, a widely applied method in facial prostheses production [57, 78]. Nevertheless, we have neglected this method, as it usually deals with a completely different kind of material namely wax. This method can

be potentially employed in further studies, concerning a comparison between wax and plastic for producing of prostheses replicas.

## 4.2 Results: dimensional accuracy

### 4.2.1 Comparison of *in vivo* data group to AM measurements: clinical relevance

Compared to the *in vivo* FDM and SL APRs showed the highest dimensional accuracy. To judge about the clinical relevance of the persisted discrepancies certain criteria must be formulated to set the threshold of their visual recognizability. According to Farkas [35] the difference of 5-mm in length and 3- to 4-mm in width are not visible for the human eye and are unlikely to have any clinical impact. Furthermore, as stated by Coward et al. [25] 2 mm difference seems to be clinically undetectable. Based on this information it can be assumed that inaccuracies up to 0.56 mm, as encountered in the present study, might not affect the general semblance of the replica and would not lead to a visible mismatch of the definitive prosthesis to the facial anatomy in general.

The maximum *relative* differences on FDM -, SLS- and SL-manufactured APRs to *in vivo* were 1.85 % (pa-pa'), -1.69 % (sba-sba') and -1.68 % (sba-sba') respectively, which exceed the threshold of 1.5 %. No comparative studies dealing with facial prostheses of their replicas were found. In the following research [3] the relative mean difference of 2 % to original coronoid process of the human mandible anatomy was concerned to be clinically not relevant. For this reason the single discrepancies in the order of  $\leq 1,85$  % seem not to influence the overall semblance of the definitive facial prostheses, although they exceed the relevant threshold set in the present study.

### 4.2.2 Comparison of CAD dataset to AM measurements

The comparison between measurements carried out on APRs and the CAD data group indicates the pure accuracy of the AM methods used in this study. Even though there would be any errors, affecting the quality of the initial virtual image, they might not be relevant for the further comparative analysis of AM methods, as far as AM-machines address to the same data source to boot up the intended 3D image. The mean *relative*

differences between CAD measurements and measurements of FDM-, SLS- and SL-produced APRs were 0.35 % 0.37 % and 0.69 % respectively, which is nearly two times less, as compared to in vivo measurements. These results indicate clearly that the stage of data gathering may affect the overall accuracy of the digital workflow of prostheses manufacturing, rather than the AM process.

In the Table 6 (page 44) groups of total relative mean differences of measurements are presented. The first one is calculated for all groups of distances – short, medium and long, whereas in the second group short distances are excluded. The reason to do this manifested itself during the process of auricular anthropometry, where the short distances sa-sa', pa-pa' and sba-sba' turned out very difficult to be measured just because some areas posterior of the auricle were simply unattainable for digital callipers. Moreover, the mentioned landmarks fell sometimes on places, which either didn't have any bony or cartilaginous support, such as "sba". Some were simply located in the haired area and must be attached to the cap, which provided the landmark with a certain degree of pliability – sa' for instance. This restricted the repeatability of the measurement. As far as it was thought that such limiting conditions might have contributed to the overall measurement accuracy, the second group of total mean differences has been calculated, neglecting thereby the short distances. Significantly lower differences up to two times between the measurements groups were found. Even so the main tendency that FDM showed the best accuracy remained unchanged.

Notwithstanding the process of data acquisition and anthropometrical measuring protocol have affected the overall accuracy of digital production workflow, the maximal mean relative difference of all AM methods to in vivo group was 0.96 %. This result is considered to be fully acceptable for the clinical application, since these dimensional changes were within the set threshold of 1,5 %. Even greater relative mean differences between AM produced models and original anatomy of the order of 2 % were thought not to have any clinical impact [3].



#### 4.2.3 Similar studies to the topic

In the topical literature only few studies have been found that investigated the dimensional accuracy of AM methods employed for APRs manufacturing. Most of them have been dealing either with cadaver skulls or dry mandibles (Table 8 – see below). It must be furthermore emphasized that all of these studies dealt with bony structures. Such circumstances differ from that ones, when investigating the reproduction accuracy of facial soft tissue parts.

Authors	Comparison	Mean differences	
		Absolute (mm)	Relative (%)
<i>Choi et al (2002)</i>	SL – CT	<b>0.57</b>	<b>0.56</b>
	SL – skull	<b>0.62</b>	<b>0.82</b>
<i>Subburaj et al (2007)</i>	FDM – CT *	<b>0.84</b>	<b>2.82</b>
<i>Silva et al (2008)</i>	SLS – skull	<b>0.89</b>	<b>2.10</b>
<i>Ibrahim et al (2009)</i>	SLS – mandible	<b>0.90</b>	<b>1.79</b>
<i>Murugesan et al (2012)</i>	FDM – mandible	–	<b>1.73</b>
<i>Shah et al (2013)</i>	FDM – CT*	<b>0.45</b>	<b>1.78</b>
The present study	Ear patterns		
	SLS – CAD**	<b>0.12</b>	<b>0.37</b>
	SLS – human ear	<b>0.25</b>	<b>0.96</b>
	FDM – CAD**	<b>0.09</b>	<b>0.35</b>
	FDM – human ear	<b>0.17</b>	<b>0.81</b>
	SL – CAD**	<b>0.13</b>	<b>0.53</b>
	SL – human ear	<b>0.19</b>	<b>0.69</b>

**Table 8. Summary of other studies on the topic of dimensional accuracy of AM methods**

\* *CT image of the human ear*

\*\* *Data acquired by means of structured light scanning*

Within the last years an ongoing improvement of FDM relative dimensional accuracy can be shown with results from 2007 reporting a relative mean difference of 2.82 % between the FDM produced APR [78], followed by 1.79 % in 2012 [62] and 1.78 % in 2013 [73]. In contrast, the present study with structured light scanning yielded 0.35 %. It must be stressed that each study mentioned above has utilized only single clinical

case. The present study covered this shortcoming with the enrolment of more participants and production of a bigger number of APRs.

The method of SLS has been also employed in a row of studies to reproduce various anatomical parts such as cadaver skulls and dry mandibles, but not ears. Some authors reported a significantly poor geometrical accuracy with mean relative differences to the original anatomy of 2.10 % and 1.79 % [49, 74]. These studies utilized CT as a source of virtual data. In the present study the mean relative difference of SLS method to in vivo measurements has been also calculated and was 0.96 %. The layer thickness used in the mentioned studies was reported to be 0.25 mm. Since 2008/09, however, the resolution of SLS method has greatly improved to more than the power of 10. The layer thickness of the machine used in the present study was 0.01 mm. This fact might have contributed also to the higher accuracy yielded in our study. No scientific researchers have been found dealing directly with the dimensional accuracy of SLS for the auricular prostheses manufacturing.

As far as the SL method is concerned, its utilization in the field of medical prototyping was also highlighted [15]. The mean relative difference of the order of 0.82 % compared to the original anatomy of human bony structure (skull) was reported, followed by only 0.56 %, when compared to the CT image. This correlates with results showed in the present study, with relative mean differences of 0.69 % and 0.53 % by in vivo and CAD measurements respectively.

#### **4.3 Results: surface structure**

According to the study of Lemperle et al. [56], facial wrinkles are 0.1 to 0.8 mm in depth. It means that the digital technologies must be capable to obtain the skin details starting from 0.1 mm. Traditionally CT scans have been used to obtain virtual images of the facial anatomy. As described in some studies [7, 31], the standard clinical scanning protocol produces the voxel size of 0.488 mm, which is clearly not enough to capture the details in the order of 0.1 mm. Although extending the scanning time or increasing the x-ray dosage may help to achieve a greater resolution of 3D images, such changes in the scanning protocol might be difficult to justify clinically. In the present study the

structured light scanner has been employed with the resolution of 0.1 mm, which was assumed to be sufficient to adequately describe the skin texture and wrinkles in the same order of 0.1 mm.

The examination of the three-dimensional image disclosed that the anatomy of the “Helix” wrinkle was no longer displayed in the CAD software, despite the resolution of the scanner was 0.1 mm, which matches the depth of a referent wrinkle with a depth of 94  $\mu$ . The unfeasibility to make the patient stay motionless during the scanning process may be responsible for this, as slight movements do restrict the accuracy of data capture.

The wrinkles “Lobula basis” and “Lobula corpus” were well visible on each APR. Visually these wrinkles were much more pronounced on the three-dimensional image, than on the stone cast. Moreover their depth, as revealed by means of the profilometrical analysis, has increased up to 45  $\mu$ m compared to the stone cast. It must be emphasized, that the depth of these wrinkles measured on the stone cast may not objectively reflect their real profile, as distortion might have occurred during the impression taking through the pressure caused by the silicone material [53, 55, 71]. The pliable ear-lobe could have been stretched, thereby smoothing up the referent wrinkles. Surface scanner in its turn, as being a non-contact technique, causes no pressure to the soft tissue. Therefore the anatomy of these wrinkles may be originally reproduced on the CAD-image. Unfortunately it was unfeasible to measure its depth faithfully in the CAD software.

Even though the method of FDM showed a sufficient level of skin details reproduction (compared to initial 3D image), the visibility of the PLA filaments may tremendously affect the overall aesthetics of the future definitive prosthesis. This problematic was highlighted in the following study – [46]. The chemical polishing was used to eliminate the staircase effect in order to acquire the smooth surface of the prosthesis. This way not only the undesired PLA filaments, but also potentially skin surface details are removed. The absolutely smooth and shiny surface varies from the characteristics of the natural skin, and therefore is questionable towards clinical acceptance.

The study of Eggbeer et al. [33] showed that the step of AM might not be a setback of the digital approach, but the stage of data acquisition. Even the accuracy of 0.02 mm was not sufficient to describe all the skin features, which ranged from 0.1 to 0.8 mm. The fact that the “Helix” wrinkle was failed to be completely reproduced on APRs can be explained rather with the scanning conditions, than with the insufficient resolution of the scanning source (0.1 in the present study). The movements of the patient caused during the scanning process and the postprocessing of the gathered data, where the gaps and errors have been filled and filtered, are responsible for the poor level of texture detailing.

#### **4.4 The potential objectives for further investigations to the topic**

The outcomes of the current trial must be applied to the clinical practice. The major concern herein would be the try-in and subsequent adjustment of the APR to the afflicted facial area. The margins of APRs must be aligned to the adjacent tissue. Difficulties may be expected, as the APRs are not made of the wax, as by the traditional approach, but of various hard materials. Their fitting may imply some trimming by means of milling tools, which may be challenging. This issue must be pursued in the further studies.

## 5 CONCLUSION

The differences between the AM-produced APRs and situation in vivo revealed in the present study are unlikely to be visually recognizable and therefore seem not to affect negatively the match of the prostheses to the adjacent tissue. In terms of dimensional accuracy all three AM methods used showed satisfactory results and are equally suitable for facial prostheses fabrication. Still the method of FDM showed the best dimensional accuracy.

The stage of data acquisition is still likely to affect the accuracy of the produced prostheses replicas rather than the accuracy of AM methods themselves. The improvement of the scanning protocol to minimize facial movements of the subjects during the scanning process is rather likely to aid the efficacy of digital prostheses manufacturing approach, than a higher resolution of the scanning device.

The complete reproduction of the skin structure details utilizing the combination of surface scanning and AM methods used in the present study was accompanied by shortcomings. Reproduction of partial surface structures was only feasible to describe the wrinkles of exceeding 192  $\mu\text{m}$  in depth. The step of data acquisition was then again responsible for this.

As far as production costs are concerned, it must be mentioned that FDM-produced APRs were much cheaper as those made by SLS and SL – quite interestingly, as it revealed the highest geometrical accuracy despite of its inferior resolution. Thus, the method of FDM showed the best trade-off between dimensional accuracy, level of texture details and pricing and can be for this reason recommended for rapid and efficient manufacturing of auricular prostheses replicas.

## 6 SUMMARY

In the current literature to the topic only little was published on the geometrical accuracy and resemblance of AM-produced prostheses replicas.

Therefore the main objective of the present study was to identify the superior AM method from FDM, SLS and SL in terms of dimensional accuracy, skin details reproduction and efficiency to produce APRs using thereby the rapid prototyping approach.

Twenty three subjects underwent a clinical study procedure encompassing ear anthropometry, followed by structured light scanning of patients' left auricles. The auricular area including the pinna was scanned with a portable surface scanner (Artec 3D Spider, Artec Group, Luxembourg, Luxembourg), utilizing the structured light scanning method. The distances of the anthropometrical landmarks were measured within the Software (ARTEC Studio, version 9), three times blinded with the "digital lineal". After the gathered data was post-processed and converted into OBJ format, it has been transferred to AM machines to produce 57 APRs by means of FDM (n=23), SLS (n=23) and SL (n=11) methods. The manufactured APRs were measured blinded three times each distance between the landmarks with the digital calipers. Measurements gathered from APRs have been compared to the In-vivo and CAD data groups. Results have been statistically evaluated.

Additionally, the surface analysis of APRs utilizing stereomicroscopy and profilometry was conducted to ascertain what level of skin details reproduction is achievable. Production costs and time were calculated.

The analysis of dimensional accuracy revealed difference up to 0.56 mm. This was found clinically acceptable, as not exceeding the threshold of 2 mm (see on page 20), which was set as a threshold ( However, the comparison of relative mean differences disclosed the bias of up to 1.85 % between the in vivo data group and AM-produced APRs, which was higher than 1.5 %, as assumed in the present study. The comparison of relative mean differences between CAD data group and APRs did not reveal any

discrepancies that may be clinically recognizable. As far as pure accuracy of AM methods is concerned, the FDM showed the best result.

The reproduction of skin surface structure was only feasible where the skin details exceed 192  $\mu\text{m}$  of depth. The reference wrinkles “Lobula basis” and “Lobula corpus” were visible on each APR. However, the wrinkle “Helix” was not reproducible by any of the employed AM methods. The FDM showed the most detailed reproduction of the tissue portion captured by means of structured light scanning. The staircase effect remains the main limiting factor of this AM method.

The disclosed differences were found to be clinically acceptable, although in 5 of 42 comparisons the mean relative differences between in vivo and APRs exceeded slightly the threshold of clinical relevance set in the present study. The step of digital data acquisition was obviously more responsible for the revealed dimensional errors than the AM methods themselves.

The method of FDM showed the best trade-off between dimensional accuracy, level of texture details and pricing. Thus FDM can be recommended for rapid and efficient manufacturing of prostheses replicas.

## 7 SUPPLEMENT

### 7.1 Attachement 1. Sample size for comparing the AM methods

Case 1.

Confidence Interval (2-sided) 95%  
 Power 80%  
 Ratio of sample size (Group 2/Group 1) 1  
 Group 1 – **Stereolithography**  
 Group 2 – **Fused deposition modeling**

---

	Group 1	Group 2	Difference*
Mean	65.95	66.07	-0.12
Standard deviation	0.1	0.12	
Variance	0.01	0.014	
Sample size of Group 1	14		
Sample size of Group 2	14		
Total sample size	28		

---

\*Difference between the means

Case 2.

Confidence Interval (2-sided) 95%  
 Power 80%  
 Ratio of sample size (Group 2/Group 1) 1  
 Group 1 – **Stereolithography**  
 Group 2 – **Selective laser sintering**

---

	Group 1	Group 2	Difference*
Mean	65.95	65.23	-0.28
Standard deviation	0.1	0.2	
Variance	0.01	0.04	
Sample size of Group 1	6		
Sample size of Group 2	6		
Total sample size	12		

---



\*Difference between the means

Case 3.

Confidence Interval (2-sided)      95%  
 Power 80%  
 Ratio of sample size (Group 2/Group 1)      1  
 Group 1 – **Fused deposition modeling**  
 Group 2 – **Selective laser sintering**

---

	Group 1	Group 2	Difference*
Mean	65.07	65.23	-0.16
Standard deviation	0.12	0.2	
Variance	0.014	0.04	
Sample size of Group 1	17		
Sample size of Group 2	17		
Total sample size	34		

## 8 ZUSAMMENFASSUNG

### 8.1 Einleitung

Erworbene und angeborene Gesichtsdefekte können mit plastischer Chirurgie häufig nicht oder nicht vollständig rekonstruiert werden. Verbleibende „Defekte“ schränken Patienten psychosozial erheblich ein. Daher werden fehlende Gesichtsanteile schon seit Jahrhunderten abgedeckt oder bestmöglich ersetzt. Heutzutage obliegt die Wiederherstellung einem Team aus chirurgischen Fächern (vor allem Mund-, Kiefer-Gesichtschirurgie, Hals-Nasen-Ohrenheilkunde) und entsprechend geschulten Personen, häufig Zahntechnikern, – sog. Epithetikern. Die so genannte Epithetik begleitet teilweise die chirurgische Rehabilitation oder steht nach dieser als abschließende Behandlung des Patienten an.

Hergestellt werden die sog. Epithesen zum Ersatz von Ohren, Nasen und Augen oder auch umfangreicheren Gesichtsversehrungen zurzeit überwiegend auf „konventionelle Art“: Das bedeutet, dass mit Hilfe einer Abformung des Defekts (anhand von irreversiblen, elastischen Abformmassen) ein 1:1 Modell aus Gips angefertigt wird. Auf diesem modelliert der Epithetiker eine Rekonstruktion aus Wachs, welche nach der Einprobe beim Patienten durch Presstechnik überführt wird in hautähnliches Silikon.

Zwei Punkte sind hier als schwierig herauszuheben:

- Die Abformung des Defekts mittels Abformmassen kann etwa durch offenliegende Schleimhäute und Körperhöhlen schmerzhaft bzw. reizend sein. Weiter besteht eine körperliche und psychische Belastung der Betroffenen, da erst „flüssiges Material“ auf und in den Körper einfließt und danach erstarrtes Material von und aus dem Körper entfernt werden muss. Bei diesem Vorgang besteht gleichwohl die Gefahr, dass die Abformung beschädigt (Abrisse von Material) und wiederholt werden muss. Darüber hinaus können die Abformmassen zu Deformationen von weichem Gewebe bei der

Abformung führen und somit kein originalgetreues Modell als Grundlage für die Modellation der Epithese liefern.

- Die Gestaltung der Rekonstruktion erfolgt „frei Hand“ durch den erfahrenen Epithetiker mit Hilfe von 2D-enface Aufnahmen des Patienten (frontal, seitlich, halbseitlich). Die dreidimensionale Passung und Harmonie im Gesicht kann erst bei der Ein-/Anprobe der Wachskonstruktion erfolgen und muss dann im Beisein des Patienten nötigenfalls geändert und gar gänzlich neu angefertigt werden.

Durch die Entwicklung von CAD/CAM Systemen ist es möglich geworden, Defekte berührungslos „virtuell“ über Laser oder Streifenlicht abzuformen bzw. aufzuzeichnen. Im Nachgang können die Defekte mittels 3D-Software im virtuellen Modell konstruiert werden. Dies ist im Computer-Assisted Design (CAD) einfach durch spiegeln und „matchen“ gesunder Areale für die Rekonstruktion möglich.

Solche 3D Modelle können mithilfe von additiven Fertigungsmethoden (AM) dem sogenannten Rapid Prototyping (RP) auf verschiedenen Wegen materialisiert werden.

### *8.1.1 Genauigkeit der AM Methoden*

Die additiven (auch generativen) Fertigungsverfahren (GVF oder Additive Manufacturing – AM) überführen 3D Modelle in Kunststoffe oder Kunstwachse. Ein „Generatives Fertigungsverfahren“ ist ein automatischer Prozess zur Herstellung maßstäblicher dreidimensionaler physischer Objekte unmittelbar aus einem 3D-CAD-Datensatz. Realisiert wird dies im „Schichtbauprinzip“: Dabei werden dreidimensionale Bauteile aus formlosem Stoff schichtweise gemäß der Kontouren des CAD-Modelles aufgebaut. Derzeit gibt es eine Vielzahl von derartigen AM-Prozessen auf dem Markt. GVF hat mehrere Anwendungsebenen, wobei solche als „Rapid Manufacturing“ (RP) und „Rapid Tooling“ (RT) im epithetischen Bereich eingesetzt werden können.

Mit RP werden die Bauteile angefertigt, um deren allgemeine Erscheinung und Proportion beurteilen zu können. Im Falle der Epithetik werden sog. Prototypen (Schablonen) hergestellt, um diese am Patienten anzuprobieren. Zu den häufig dafür

verwendeten RP-Verfahren gehören das Stereolithographische Verfahren (SL), das Selektive Lasersintern (SLS) und das Fused Deposit Modelling (FDM).

Die technische Genauigkeit von den oben genannten Methoden ist in der Literatur bereits gut beschrieben. Jedoch wurde bis jetzt nicht untersucht, welches dieser Verfahren für die Herstellung von Gesichtsprothesen im Sinn der Präzision und Reproduzierbarkeit von anthropometrischen Formen und Ankerpunkten am besten geeignet ist. Das Ohr ist die komplexeste 3D-Struktur des menschlichen Gesichts. Gleichzeitig bietet das Ohr den Vorteil, sich mimisch/muskulär unwillkürlich nicht oder nur sehr bedingt zu bewegen. Weiter liegen in der Literatur bereits anthropometrische Landmarks bei Ohren vor, welche als Referenzpunkte zu Vermessung herangezogen werden können. In dieser Studie haben wir das anthropometrische Protokoll nach Farkas benutzt, wobei noch zwei zusätzliche Messpunkte von Coward hinzugefügt wurden.

Es bleibt also fraglich, in welcher Genauigkeit die Umsetzung komplexer anatomischer Strukturen mittels CAD/CAM und RP Systemen möglich ist.

### *8.1.2 Reproduzierbarkeit der Hautstruktur*

Um die Epithese möglichst unauffällig zu gestalten, muss diese nicht nur von den Dimensionen her genau sein, sondern auch eine ähnliche/ gleiche Struktur des ursprünglichen und angrenzenden Gewebes aufweisen. Die Erfassung aller Details der Hautoberfläche mittels 3D-Scanner ist heutzutage bedingt möglich. Die Auflösung der meisten Scangeräte beträgt 0.1 mm. Diese Genauigkeit müsste ausreichend sein, um die Faltenanatomie von 0.1 mm in der Tiefe aufzunehmen. Die Falten, die mit dem Auge erkennbar sind, liegen im Bereich von 0.1 bis 0.8 mm [56]. Obgleich moderne Bildgebungsmethoden in der Lage sind, ein gutes 3D Bild von dem zu ersetzenden Organ zu liefern, können bereits Bewegungen des Patienten oder auch die Übertragung mit AM zu Qualitätsverlust führen. Es ist also noch unklar, inwieweit Erfassung und AM in der Lage sind Hautstrukturen zu reproduzieren.

### 8.1.3 *Zweck der Studie*

Erforschung der Dimensions- und Reproduziergenauigkeit von drei AM-Verfahren zur Herstellung von Gesichtsprothesen am Beispiel von menschlichen Ohren

### 8.1.4 *Ziel der Studie*

Die Erkenntnisse sollen helfen, ein geeignetes System für die Anfertigung von epithetischen Rekonstruktionen empfehlen zu können. Die Ergebnisse helfen den Stellenwert digitaler Abform- und Herstellungsmethoden in der Epithetik zu umreißen und geben eine Aussicht auf die mögliche Entlastung des Patienten (Abformung), des Epithetikers (Herstellungsprozess) sowie langfristig der Krankenkassen (Herstellungskosten).

### 8.1.5 *Wissenschaftliche Hypothesen*

1. Es gibt keine klinisch relevanten Unterschiede zwischen in vivo Datensatz und Messungen von FDM- SLS- und SL-hergestellten Ohrschablonen
2. Es gibt keine klinisch relevanten Unterschiede zwischen CAD Datensatz und Messungen von FDM- SLS- und SL-hergestellten Ohrschablonen
3. Die in dieser Studie eingesetzten AM-Methoden in Kombination mit dem Streifenlichtscanner lassen die Hautstruktur auf den angefertigten Ohrschablonen vollkommen reproduzieren (Falten ab 0.1 mm in der Tiefe sind reproduzierbar).
4. Anhand von Abwägung von Kosten, Genauigkeit und Oberflächenbeschaffenheit ist es möglich, die „best-in-practice“ AM Methode zu identifizieren

## 8.2 **Probanden, Materialien und Methoden**

Alle eingesetzten Geräte und Materialien sind zur Verwendung am Menschen zugelassen. Der Prüfplan sowie die Aufklärung und Einverständnisunterlagen für

Probanden wurden von der Ethikkommission des Universitätsklinikums Tübingen beraten und genehmigt (#387/2014BO2).

#### *8.2.1 Rekrutierung und Erfassung von Probanden (in vivo)*

Es wurden 23 unversehrte Ohren von 23 rekrutierten, gesunden Probanden (Alter 18-60 Jahre) mittels Lichtscanner (Strukturlicht) sowie analoger Vermessung anonymisiert erfasst. Für die Untersuchung wurden die Ohren an jeweils elf Referenzpunkten mit 1 mm großen Kügelchen markiert werden. Die Fixierung der Kügelchen erfolgte durch handelsüblichen Hautkleber, welcher einfach wieder abgewaschen werden kann. Die Abstände der Referenzpunkte wurden mittels digitalen Messschiebers am Ohr des Patienten vermessen. Jede Messung wurde zur Bestimmung des Messfehlers dreimal verblindet durchgeführt. Im Anschluss erfasste der Artec Scanner Spider der Firma Artec Group mit 3D-Strukturlicht das Ohr des Patienten.

#### *8.2.2 Produktionsphase*

Die virtuellen Daten wurden am PC so bearbeitet (Artec Studio), dass diese mit allen RP-Verfahren (STL, SLS, FDM) alio loco angefertigt werden konnten.

#### *8.2.3 Referenzmessung (CAD, STL, FDM, SL)*

Die Referenzpunkte bleiben im 3-D Datensätzen sowie auf den RP Modellen erhalten. In der Software erfolgte die Vermessung ebenso dreimal verblindet mit dem integrierten Messtool. Die AM Modelle wurden analog zur in vivo Messung mittels digitalem Messschieber je Messpunkt dreimal verblindet vermessen.

#### *8.2.4 Statistische Methode*

Die alle Messdatensätze von CAD und Modellen wurden mit in-vivo Datensätzen verglichen. Dazu erfolgt die Berechnung des Messfehlers aller Erhebungen. Bei vergleichbaren Messfehlern wurden die Abweichungen zwischen den Messreihen (in-vivo, CAD, STL, SL, FDM) mittels Bland-Altman-Plot berechnet.

Eine Abweichung der Genauigkeit von 1.5 % in Bezug auf den Goldstandard (in-vivo-Messung) in einer Ebene wurde als klinisch relevant angenommen. Die Bewertung „best in practice“ erfolgt aus dem Scoring von maximaler Abweichung (Primärparameter), Qualitativer Oberflächenuntersuchung (Sekundärparameter) und Herstellungskosten.

### 8.2.5 *Hautstruktur*

Um die Reproduktion der Hautstruktur der AM-Methoden und 3D-Scanner beurteilen zu können, wurde ein Stereomikroskopietest (WILD 400, Heeburg, Schweiz) und Profilometrie (Perthometer S6P, Mahr, Goettingen, Deutschland) durchgeführt. Die zwei Referenzzonen wurden ausgewählt („Helix“ und „Lobula“), die anschließend durch das Mikroskop geprüft wurden. Für den profilometrischen Test sind drei Falten auf der Ohroberfläche ausgesucht worden („Helix“, „Lobula basis“, „Lobula corpus“), deren Tiefe gemessen wurde. Als Goldstandard wurde das Gipsmodell eines individuellen Ohres (erhalten durch Abformung) verwendet.

## 8.3 **Ergebnisse**

Die Genauigkeitsanalyse der verwendeten AM-Methoden hat die Hypothese 1 und 2 angenommen. Die mittlere prozentuale Abweichung von FDM, SLS und SL zu in vivo war jeweils 0.81, 0.96 und 0.69 %. Wenn man aber von den kurzen Distanzen absieht, die die meisten Messfehler erzeugt haben, so weist die FDM Methode die beste Genauigkeit auf mit der prozentualen Abweichung von 0.43 %, gefolgt von SLS (0.54 %) und SL (0.59 %). Die mittlere Abweichung der Messstrecken von CAD zu FDM, SLS und SL war 0.35 %, 0.37 % und 0.53 %. Die FDM Methode zeigte die beste Dimensionswiedergabe.

Es muss berücksichtigt werden, dass bei Messung der kurzen Strecken (Ohrabstand vom Kopf) vergleichsweise erhöhte Ungenauigkeiten (Messfehler) vorlagen. Ohne die kurzen Strecken zeigt das FDM-Verfahren die beste Dimensionswiedergabe verglichen sowohl mit in vivo als auch mit CAD.

Die Hypothese 3 wurde widerlegt. Obwohl die Stereomikroskopie ähnliche Oberflächen liefert wie das Gipsmodell war, ergab die Profilometrie, dass die Falten von 0.1 mm in der Tiefe nicht von dem 3D-Scanner erfasst und ebenso nicht von den verwendeten AM-Methoden reproduziert werden konnten.

Abschließend war es möglich in Abwägung von Kosten, Genauigkeit und Oberflächenbeschaffenheit, die FDM Methode als „best-in-practice“ zu identifizieren.



## **9 PUBLICATIONS**

On the 1<sup>st</sup> June 2016 the manuscript of the paper with the results of the present study was submitted by the Nature Scientific Reports journal (SREP-16-19861).

The results of the study were presented within the 40<sup>th</sup> European Prosthodontic Association (EPA) and 65<sup>th</sup> German Society for Prosthetic Dentistry and Biomaterials (DGPro) on the 17<sup>th</sup> of September and will be published in the abstract book.

## 10 REFERENCE

1. Al Mardini, M., C. Ercoli, and G.N. Graser (2005) *A technique to produce a mirror-image wax pattern of an ear using rapid prototyping technology*. *J Prosthet Dent* 94 (2): p. 195-8. DOI: 10.1016/j.prosdent.2005.04.019
2. Altman, D.G. (1991) *Altman Practical Statistics in Medicine, Reprint 1993, 1st Edition 1991; 122-151*. Boca Raton, Florida: CRC Press.
3. Asaumi, J., N. Kawai, Y. Honda, H. Shigehara, T. Wakasa, and K. Kishi (2001) *Comparison of three-dimensional computed tomography with rapid prototype models in the management of coronoid hyperplasia*. *Dentomaxillofac Radiol* 30 (6): p. 330-5. DOI: 10.1038/sj/dmfr/4600646
4. Barker, T.M., W.J. Earwaker, and D.A. Lisle (1994) *Accuracy of stereolithographic models of human anatomy*. *Australas Radiol* 38 (2): p. 106-11.
5. Berry, E., J.M. Brown, M. Connell, C.M. Craven, N.D. Efford, A. Radjenovic, and M.A. Smith (1997) *Preliminary experience with medical applications of rapid prototyping by selective laser sintering*. *Med Eng Phys* 19 (1): p. 90-6.
6. Beumer, J., T.A. Curtis, and M.T. Marunick (1996) *Maxillofacial Rehabilitation: Prosthodontic and Surgical Considerations; 328-333*. St. Louis, Toronto, London: The C.V. Mosby Company.
7. Bibb, R., D. Eggbeer, and P. Evans (2010) *Rapid prototyping technologies in soft tissue facial prosthetics: current state of the art*. *Rapid Prototyping Journal* 16 (2): p. 130-137. DOI: doi:10.1108/13552541011025852
8. Bland, J.M. and D.G. Altman (1996) *Measurement error and correlation coefficients*. *BMJ* 313 (7048): p. 41-2.
9. Bland, J.M. and D.G. Altman (1999) *Measuring agreement in method comparison studies*. *Statistical Methods in Medical Research* 8 (2): p. 135-160. DOI: 10.1177/096228029900800204
10. Brinkmann, B. and D.I.N. V (2012) *Internationales Wörterbuch der Metrologie: Grundlegende und allgemeine Begriffe und zugeordnete Benennungen (VIM) Deutsch-englische Fassung ISO/IEC-Leitfaden 99:2007*. Berlin: Beuth Verlag GmbH.
11. Chandra, A., J. Watson, J. Rowson, L. Cheng, R. Darlison, A. Sibtain, J. Holland, R. Harris, and D.J. Williams (2005) *Application of rapid manufacturing techniques in support of maxillofacial treatment—Evidence of the requirements of clinical applications*. *International Journal of Oral and Maxillofacial Surgery* 34: p. 38. DOI: 10.1016/S0901-5027(05)81017-3
12. Cheah, C.M., C.K. Chua, and K.H. Tan (2003) *Integration of laser surface digitizing with CAD/CAM techniques for developing facial prostheses. Part 2: Development of molding techniques for casting prosthetic parts*. *Int J Prosthodont* 16 (5): p. 543-8.

13. Cheah, C.M., C.K. Chua, K.H. Tan, and C.K. Teo (2003) *Integration of laser surface digitizing with CAD/CAM techniques for developing facial prostheses. Part 1: Design and fabrication of prosthesis replicas*. *Int J Prosthodont* 16 (4): p. 435-41.
14. Chen, L.H., S. Tsutsumi, and T. Iizuka (1997) *A CAD/CAM technique for fabricating facial prostheses: a preliminary report*. *Int J Prosthodont* 10 (5): p. 467-72.
15. Choi, J.Y., J.H. Choi, N.K. Kim, Y. Kim, J.K. Lee, M.K. Kim, J.H. Lee, and M.J. Kim (2002) *Analysis of errors in medical rapid prototyping models*. *Int J Oral Maxillofac Surg* 31 (1): p. 23-32. DOI: 10.1054/ijom.2000.0135
16. Ciocca, L., G. Bacci, R. Mingucci, and R. Scotti (2009) *CAD-CAM construction of a provisional nasal prosthesis after ablative tumour surgery of the nose: a pilot case report*. *Eur J Cancer Care (Engl)* 18 (1): p. 97-101. DOI: 10.1111/j.1365-2354.2008.01013.x
17. Ciocca, L., F. De Crescenzo, M. Fantini, and R. Scotti (2010) *Rehabilitation of the nose using CAD/CAM and rapid prototyping technology after ablative surgery of squamous cell carcinoma: a pilot clinical report*. *Int J Oral Maxillofac Implants* 25 (4): p. 808-12.
18. Ciocca, L., M. Fantini, C. Marchetti, R. Scotti, and C. Monaco (2010) *Immediate facial rehabilitation in cancer patients using CAD-CAM and rapid prototyping technology: a pilot study*. *Support Care Cancer* 18 (6): p. 723-8. DOI: 10.1007/s00520-009-0676-5
19. Ciocca, L., R. Mingucci, G. Gassino, and R. Scotti (2007) *CAD/CAM ear model and virtual construction of the mold*. *J Prosthet Dent* 98 (5): p. 339-43. DOI: 10.1016/s0022-3913(07)60116-4
20. Ciocca, L. and R. Scotti (2004) *CAD-CAM generated ear cast by means of a laser scanner and rapid prototyping machine*. *J Prosthet Dent* 92 (6): p. 591-5. DOI: 10.1016/s0022391304005542
21. Ciocca, L. and R. Scotti (2014) *Oculo-facial rehabilitation after facial cancer removal: updated CAD/CAM procedures. A pilot study*. *Prosthet Orthot Int* 38 (6): p. 505-9. DOI: 10.1177/0309364613512368
22. Coleman, A.J., J.W. Schweiger, J. Urquiola, and K.A. Tompkins (1995) *A two-stage impression technique for custom facial prostheses*. *J Prosthet Dent* 73 (4): p. 370-2.
23. Coward, T.J., B.J. Scott, R.M. Watson, and R. Richards (2002) *Identifying the position of an ear from a laser scan: the significance for planning rehabilitation*. *Int J Oral Maxillofac Surg* 31 (3): p. 244-51. DOI: 10.1054/ijom.2001.0152
24. Coward, T.J., B.J. Scott, R.M. Watson, and R. Richards (2005) *A comparison between computerized tomography, magnetic resonance imaging, and laser scanning for capturing 3-dimensional data from an object of standard form*. *Int J Prosthodont* 18 (5): p. 405-13.
25. Coward, T.J., B.J. Scott, R.M. Watson, and R. Richards (2006) *A comparison between computerized tomography, magnetic resonance imaging, and laser scanning for capturing 3-dimensional data from a natural ear to aid rehabilitation*. *Int J Prosthodont* 19 (1): p. 92-100.

26. Coward, T.J., B.J. Scott, R.M. Watson, and R. Richards (2007) *A comparison of prosthetic ear models created from data captured by computerized tomography, magnetic resonance imaging, and laser scanning*. *Int J Prosthodont* 20 (3): p. 275-85.
27. Coward, T.J., R.M. Watson, R. Richards, and B.J. Scott (2012) *A comparison of three methods to evaluate the position of an artificial ear on the deficient side of the face from a three-dimensional surface scan of patients with hemifacial microsomia*. *Int J Prosthodont* 25 (2): p. 160-5.
28. Davis, B.K. (2010) *The role of technology in facial prosthetics*. *Curr Opin Otolaryngol Head Neck Surg* 18 (4): p. 332-40. DOI: 10.1097/MOO.0b013e32833bb38c
29. De Crescenzo, F., M. Fantini, L. Ciocca, F. Persiani, and R. Scotti (2011) *Design and manufacturing of ear prosthesis by means of rapid prototyping technology*. *Proc Inst Mech Eng H* 225 (3): p. 296-302.
30. Dean AG, S.K., Soe MM (2015) *OpenEpi: Open Source Epidemiologic Statistics for Public Health*. [http://www.openepi.com/Menu/OE\\_Menu.html](http://www.openepi.com/Menu/OE_Menu.html) [Zugriff 10.03.14].
31. Eggbeer, D., R. Bibb, and P. Evans (2004) *Orbital prosthesis wax pattern production using computer aided design and rapid prototyping techniques*.
32. Eggbeer, D., R. Bibb, and P. Evans (2006) *Toward identifying specification requirements for digital bone-anchored prosthesis design incorporating substructure fabrication: a pilot study*. *Int J Prosthodont* 19 (3): p. 258-63.
33. Eggbeer, D., P.L. Evans, and R. Bibb (2006) *A pilot study in the application of texture relief for digitally designed facial prostheses*. *Proc Inst Mech Eng H* 220 (6): p. 705-14.
34. Ehring, F. and Fachklinik (1985) *Die Epithese zur Rehabilitation des Gesichtsversehrten: Ergebnisse der Arbeitstagung anlässlich des 50jährigen Bestehens der Fachklinik Hornheide in Münster-Handorf*. Quintessenz Verlag.
35. Farkas, L.G. (1978) *Anthropometry of normal and anomalous ears*. *Clin Plast Surg* 5 (3): p. 401-12.
36. Farkas, L.G. (1994) *Anthropometry of the head and face*. New York: Raven Press.
37. Fastermann, P. (2014) *3D-Drucken: Wie die generative Fertigungstechnik funktioniert*. Berlin, Heidelberg: Springer
38. Federspil, P.A. (2010) *Auricular prostheses*. *Adv Otorhinolaryngol* 68: p. 65-80. DOI: 10.1159/000314563
39. Feng, Z., Y. Dong, Y. Zhao, S. Bai, B. Zhou, Y. Bi, and G. Wu (2010) *Computer-assisted technique for the design and manufacture of realistic facial prostheses*. *Br J Oral Maxillofac Surg* 48 (2): p. 105-9. DOI: 10.1016/j.bjoms.2009.05.009
40. Fourie, Z., J. Damstra, P.O. Gerrits, and Y. Ren (2011) *Evaluation of anthropometric accuracy and reliability using different three-dimensional scanning systems*. *Forensic Sci Int* 207 (1-3): p. 127-34. DOI: 10.1016/j.forsciint.2010.09.018
41. Gebhardt, A. (2014) *3D-Drucken: Grundlagen und Anwendungen des Additive Manufacturing (AM)*. München: Hanser Fachbuchverlag.

42. Germec-Cakan, D., H.I. Canter, B. Nur, and T. Arun (2010) *Comparison of facial soft tissue measurements on three-dimensional images and models obtained with different methods*. J Craniofac Surg 21 (5): p. 1393-9. DOI: 10.1097/SCS.0b013e3181ec6976
43. Gion, G.G. (2006) *Surgical versus prosthetic reconstruction of microtia: the case for prosthetic reconstruction*. J Oral Maxillofac Surg 64 (11): p. 1639-54. DOI: 10.1016/j.joms.2006.03.050
44. Hagl, R. (2015) *3D-Druck-Technologien, 15-37. Das 3D-Druck-Kompodium*. Wiesbaden: Springer Fachmedien.
45. Hatamleh, M.M. and J. Watson (2013) *Construction of an implant-retained auricular prosthesis with the aid of contemporary digital technologies: a clinical report*. J Prosthodont 22 (2): p. 132-6. DOI: 10.1111/j.1532-849X.2012.00916.x
46. He, Y., G.H. Xue, and J.Z. Fu (2014) *Fabrication of low cost soft tissue prostheses with the desktop 3D printer*. Sci Rep 4: p. 6973. DOI: 10.1038/srep06973
47. Holberg, C., K. Schwenzer, L. Mahaini, and I. Rudzki-Janson (2006) *Accuracy of facial plaster casts*. Angle Orthod 76 (4): p. 605-11. DOI: 10.1043/0003-3219(2006)076[0605:aofpc]2.0.co;2
48. Hull, C.W. (1986) *Apparatus for production of three-dimensional objects by stereolithography*. Google Patents.
49. Ibrahim, D., T.L. Broilo, C. Heitz, M.G. de Oliveira, H.W. de Oliveira, S.M. Nobre, J.H. Dos Santos Filho, and D.N. Silva (2009) *Dimensional error of selective laser sintering, three-dimensional printing and PolyJet models in the reproduction of mandibular anatomy*. J Craniomaxillofac Surg 37 (3): p. 167-73. DOI: 10.1016/j.jcms.2008.10.008
50. Jiao, T., F. Zhang, X. Huang, and C. Wang (2004) *Design and fabrication of auricular prostheses by CAD/CAM system*. Int J Prosthodont 17 (4): p. 460-3.
51. Jindal, S.K., M. Sherriff, M.G. Waters, and T.J. Coward (2016) *Development of a 3D printable maxillofacial silicone: Part I. Optimization of polydimethylsiloxane chains and cross-linker concentration*. J Prosthet Dent. DOI: 10.1016/j.prosdent.2016.02.020
52. Karakoca, S., C. Aydin, H. Yilmaz, and T. Korkmaz (2008) *An impression technique for implant-retained orbital prostheses*. J Prosthet Dent 100 (1): p. 52-5. DOI: 10.1016/s0022-3913(08)60137-7
53. Kubon, T.M. and J.D. Anderson (2003) *An implant-retained auricular impression technique to minimize soft tissue distortion*. J Prosthet Dent 89 (1): p. 97-101. DOI: 10.1067/mpr.2003.16
54. Larsson, J. (2015) *Additive und hybride Produktion mit 3D-Druck [online]* [http://www.x-technik.at/downloads/flipbook/additive\\_fertigung/2015/AF\\_01\\_2015\\_screen.pdf](http://www.x-technik.at/downloads/flipbook/additive_fertigung/2015/AF_01_2015_screen.pdf) [Zugriff 11.06.16]. Additive Fertigung, 26-31.
55. Lemon, J.C., D.J. Okay, J.M. Powers, J.W. Martin, and M.S. Chambers (2003) *Facial mouldage: the effect of a retarder on compressive strength and working and setting times of irreversible hydrocolloid impression material*. J Prosthet Dent 90 (3): p. 276-81. DOI: 10.1016/s0022391303003664

56. Lemperle, G., R.E. Holmes, S.R. Cohen, and S.M. Lemperle (2001) *A classification of facial wrinkles*. *Plast Reconstr Surg* 108 (6): p. 1735-50; discussion 1751-2.
57. Liacouras, P., J. Garnes, N. Roman, A. Petrich, and G.T. Grant (2011) *Designing and manufacturing an auricular prosthesis using computed tomography, 3-dimensional photographic imaging, and additive manufacturing: a clinical report*. *J Prosthet Dent* 105 (2): p. 78-82. DOI: 10.1016/s0022-3913(11)60002-4
58. Lill, W., P. Solar, C. Ulm, G. Watzek, R. Blahout, and M. Matejka (1992) *Reproducibility of three-dimensional CT-assisted model production in the maxillofacial area*. *Br J Oral Maxillofac Surg* 30 (4): p. 233-6.
59. Littlefield, T.R., K.M. Kelly, J.C. Cherney, S.P. Beals, and J.K. Pomatto (2004) *Development of a new three-dimensional cranial imaging system*. *J Craniofac Surg* 15 (1): p. 175-81.
60. Marafon, P.G., B.S. Mattos, A.C. Saboia, and P.Y. Noritomi (2010) *Dimensional accuracy of computer-aided design/computer-assisted manufactured orbital prostheses*. *Int J Prosthodont* 23 (3): p. 271-6.
61. Murphy, S.V. and A. Atala (2014) *3D bioprinting of tissues and organs*. *Nat Biotechnol* 32 (8): p. 773-85. DOI: 10.1038/nbt.2958
62. Murugesan, K., P.A. Anandapandian, S.K. Sharma, and M. Vasantha Kumar (2012) *Comparative evaluation of dimension and surface detail accuracy of models produced by three different rapid prototype techniques*. *J Indian Prosthodont Soc* 12 (1): p. 16-20. DOI: 10.1007/s13191-011-0103-8
63. Palousek, D., J. Rosicky, and D. Koutny (2014) *Use of digital technologies for nasal prosthesis manufacturing*. *Prosthet Orthot Int* 38 (2): p. 171-5. DOI: 10.1177/0309364613489333
64. Petzold, R., H.F. Zeilhofer, and W.A. Kalender (1999) *Rapid prototyping technology in medicine--basics and applications*. *Comput Med Imaging Graph* 23 (5): p. 277-84.
65. Pfütz, E. (1970) *Untersuchungen zu den Problemen der epithetischen Defektdeckung im Kopfbereich und ihre Lösung durch moderne Verfahren. Medizinische Habilitationsschrift. Philipps-Universität Marburg*.
66. Qiu, J., X.Y. Gu, Y.Y. Xiong, and F.Q. Zhang (2011) *Nasal prosthesis rehabilitation using CAD-CAM technology after total rhinectomy: a pilot study*. *Support Care Cancer* 19 (7): p. 1055-9. DOI: 10.1007/s00520-011-1157-1
67. Rahn, A.O. and L.J. Boucher (1970) *Maxillofacial Prosthetics: Principles and Concepts*. Philadelphia: Saunders.
68. Richard, B., E. Dominic, and E. Peter (2010) *Rapid prototyping technologies in soft tissue facial prosthetics: current state of the art*. *Rapid Prototyping Journal* 16 (2): p. 130-137. DOI: 10.1108/13552541011025852
69. Roberts, A.C. (1971) *Facial Prostheses: The Restoration of Facial Defects by Prosthetic Means*. Kimpton.

70. Runte, C., D. Dirksen, H. Delere, C. Thomas, B. Runte, U. Meyer, G. von Bally, and F. Bollmann (2002) *Optical data acquisition for computer-assisted design of facial prostheses*. *Int J Prosthodont* 15 (2): p. 129-32.
71. Sabol, J.V., G.T. Grant, P. Liacouras, and S. Rouse (2011) *Digital image capture and rapid prototyping of the maxillofacial defect*. *J Prosthodont* 20 (4): p. 310-4. DOI: 10.1111/j.1532-849X.2011.00701.x
72. Schwenzer, N. (1994) *Prothetik und Werkstoffkunde*. Stuttgart: G. Thieme.
73. Shah, M. (2013) *RETRACTED: Auricular prosthesis fabrication using computer-aided design and rapid prototyping technologies*. *Prosthet Orthot Int*. DOI: 10.1177/0309364613504779
74. Silva, D.N., M. Gerhardt de Oliveira, E. Meurer, M.I. Meurer, J.V. Lopes da Silva, and A. Santa-Barbara (2008) *Dimensional error in selective laser sintering and 3D-printing of models for craniomaxillary anatomy reconstruction*. *J Craniomaxillofac Surg* 36 (8): p. 443-9. DOI: 10.1016/j.jcms.2008.04.003
75. Stansbury, J.W. and M.J. Idacavage (2015) *3D printing with polymers: Challenges among expanding options and opportunities*. *Dent Mater*. DOI: 10.1016/j.dental.2015.09.018
76. Staudenmaier, R., N.T. Hoang, V. Mandlik, C. Schurr, M. Burghartz, K. Hauber, G. Meier, G. Kadegge, and T. Blunk (2010) *Customized tissue engineering for ear reconstruction*. *Adv Otorhinolaryngol* 68: p. 120-31. DOI: 10.1159/000314567
77. Sterodimas, A., J. de Faria, W.E. Correa, and I. Pitanguy (2009) *Tissue engineering and auricular reconstruction: a review*. *J Plast Reconstr Aesthet Surg* 62 (4): p. 447-52. DOI: 10.1016/j.bjps.2008.11.046
78. Subburaj, K., C. Nair, S. Rajesh, S.M. Meshram, and B. Ravi (2007) *Rapid development of auricular prosthesis using CAD and rapid prototyping technologies*. *Int J Oral Maxillofac Surg* 36 (10): p. 938-43. DOI: 10.1016/j.ijom.2007.07.013
79. Sykes, L.M., A.M. Parrott, C.P. Owen, and D.R. Snaddon (2004) *Applications of rapid prototyping technology in maxillofacial prosthetics*. *Int J Prosthodont* 17 (4): p. 454-9.
80. Taylor, T.D. (2000) *Clinical Maxillofacial Prosthetics*. Chicago, London: Quintessence Publishing Company.
81. Tsuji, M., N. Noguchi, K. Ihara, Y. Yamashita, M. Shikimori, and M. Goto (2004) *Fabrication of a maxillofacial prosthesis using a computer-aided design and manufacturing system*. *J Prosthodont* 13 (3): p. 179-83. DOI: 10.1111/j.1532-849X.2004.04029.x
82. Turgut, G., B. Sacak, K. Kiran, and L. Bas (2009) *Use of rapid prototyping in prosthetic auricular restoration*. *J Craniofac Surg* 20 (2): p. 321-5. DOI: 10.1097/SCS.0b013e3181992266
83. Volkenstein, S., S. Dazert, K. Jahnke, M. Schneider, and A. Neumann (2007) *Prosthetic supply of tissue defects in head and neck surgery*. *Laryngorhinootologie* 86 (12). DOI: 10.1055/s-2007-966888
84. Watson, J. and M.M. Hatamleh (2014) *Complete integration of technology for improved reproduction of auricular prostheses*. *J Prosthet Dent* 111 (5): p. 430-6. DOI: 10.1016/j.prosdent.2013.07.018

85. Webb, P.A. (2000) *A review of rapid prototyping (RP) techniques in the medical and biomedical sector*. J Med Eng Technol 24 (4): p. 149-53.
86. Winder, J. and R. Bibb (2005) *Medical rapid prototyping technologies: state of the art and current limitations for application in oral and maxillofacial surgery*. J Oral Maxillofac Surg 63 (7): p. 1006-15.
87. Wong, J.Y., A.K. Oh, E. Ohta, A.T. Hunt, G.F. Rogers, J.B. Mulliken, and C.K. Deutsch (2008) *Validity and reliability of craniofacial anthropometric measurement of 3D digital photogrammetric images*. Cleft Palate Craniofac J 45 (3): p. 232-9. DOI: 10.1597/06-175
88. Wu, G., B. Zhou, Y. Bi, and Y. Zhao (2008) *Selective laser sintering technology for customized fabrication of facial prostheses*. J Prosthet Dent 100 (1): p. 56-60. DOI: 10.1016/s0022-3913(08)60138-9
89. Yoshioka, F., S. Ozawa, S. Okazaki, and Y. Tanaka (2010) *Fabrication of an orbital prosthesis using a noncontact three-dimensional digitizer and rapid-prototyping system*. J Prosthodont 19 (8): p. 598-600. DOI: 10.1111/j.1532-849X.2010.00655.x



## **11 DECLARATION OF THE OWN SHARE TO THIS STUDY**

With these lines I (further on as investigator indicated) would like to declare my contribution to the performed scientific work.

The idea to investigate the methods of medical rapid prototyping in the field of maxillofacial prosthetics manifested itself in 2011 during the probation period in the Department of Prosthetic Dentistry of the University of Tuebingen, as far as the investigator was dealt with patients suffering from facial disfigurements in cooperation with the skillful dental technician that has been working in the mentioned department. Later on the head of the Department of Prosthetic Dentistry, Professor Dr. H. Weber set the final topic of the future scientific research.

The review of the current topical literature has been conducted in November 2011 in the University of Tuebingen and lasted till recent time due to the big number of publication on this topic. This review has been performed by the investigator.

The study protocol was written by the investigator in the year of 2012 in order to apply for the scholarship to the Ministry of Science and Education of Russian Federation. The application was submitted in May of 2013 which resulted in foundation of this study and the further post-graduate study within the wall of the Department of Prosthodontics of the University of Tuebingen.

During the pilot-phase senior associates PD Dr. E. Engel and Dr. F. Huettig did contribute greatly to the refinement of the study protocol and trouble-free carry out of the research.

During the study the investigator performed the anthropometrical analysis of the probands' auricles, the gathering of the three-dimensional images by means of structured light scanning, as well as made the postprocessing, editing and refinement of the collected CAD-data in special software. As special class at the official reseller has been taken in order to learn how the surface scanner must be dealt with and to obtain high-quality renderings.

The manufacturing of the auricular prosthesis prototypes has been performed within the outsourcing partnership with several firms dealing with AM under the supervision of the investigator.

The surface structure analysis and profilometry were held in cooperation with B.Sc. S. Spintzyk.

Afterwards the anthropometrical analysis of the manufactured auricular patters has been carried out by the investigator. The data has been statistically evaluated in cooperation with the senior associate Dr. F. Huettig

The whole research in general has been supervised by the head of the Department of Prosthetic Dentistry of the University of Tuebingen Prof. Dr. H. Weber and senior associates PD Dr. E. Engel and Dr. F. Huettig.

On the 1<sup>st</sup> June 2016 the results of the present study was submitted by the Nature Scientific Reports journal (SREP-16-19861).

The results of the study were presented within the 40<sup>th</sup> European Prosthodontic Association (EPA) and 65<sup>th</sup> German Society for Prosthetic Dentistry and Biomaterials (DGPro) on the 17<sup>th</sup> of September and will be published in the abstract book.

## **12 ACKNOWLEDGMENTS**

First of all I would like to thank the head of the Department of Prosthetic Dentistry of the University of Tuebingen, Professor Dr. Heiner Weber for the granted opportunity to be the doctoral student at his department, for his guidance throughout my scientific work and his ideas to the topic he shared with me.

Further on I would like to express my sincere gratitude to my advisor Priv.-Doz. Dr. E. Engel for her continuous support of my study and related research and for her guidance while writing of this thesis.

Also I would like to thank Dr. F. Huettig for his insightful comments, encouragement and advice while performing this study.

My sincere thanks also goes to Prof. Dr. J. Geis-Gerstorfer and S. Spintzyk B. Sc., who provided me an opportunity to join their team, and who gave access to the laboratory and research facilities.

The present study was financed by the scholarship of the Ministry of Education and Science of Russian Federation and also by the Department of Prosthodontics in the Center of Dentistry, Oral Medicine and Maxillofacial Surgery of the University of Tuebingen.

### 13 CURRICULUM VITAE

Name	Alexey Sergejewitsch Unkovskiy
Date of birth	04.01.1990
Place of birth	Moscow (USSR)
Nationality	Russian
Education:	
September 1996 – June 2005	Gymnasium school in Russia
September 2005 – June 2010	Study of Dentistry in Moscow State University of Medicine and Dentistry. Diploma with honours.
September 2010 – June 2011	Clinical Residency for Dentistry of General practice
September 2011 – June 2013	Clinical Residency for Prosthetic Dentistry
Since October 2013	Doctoral student at the University of Tuebingen, Department of Prosthodontics